Commun. Comput. Phys.
doi: 10.4208/cicp.250614.060215a

Vol. **18**, No. 3, pp. 673-706
September 2015

Effect of Geometric Conservation Law on Improving Spatial Accuracy for Finite Difference Schemes on Two-Dimensional Nonsmooth Grids

Meiliang Mao[1,2,*], Huajun Zhu[1], Xiaogang Deng[3], Yaobing Min[1] and Huayong Liu[1]

[1] *State Key Laboratory of Aerodynamics, CARDC, Mianyang, 621000, P.R. China.*
[2] *Computational Aerodynamics Institute, CARDC, Mianyang, 621000, P.R. China.*
[3] *National University of Defense Technology, Changsha, Hunan, 410073, P.R. China.*

Communicated by Chi-Wang Shu

Received 25 June 2014; Accepted (in revised version) 6 February 2015

Abstract. It is well known that grid discontinuities have significant impact on the performance of finite difference schemes (FDSs). The geometric conservation law (GCL) is very important for FDSs on reducing numerical oscillations and ensuring free-stream preservation in curvilinear coordinate system. It is not quite clear how GCL works in finite difference method and how GCL errors affect spatial discretization errors especially in nonsmooth grids. In this paper, a method is developed to analyze the impact of grid discontinuities on the GCL errors and spatial discretization errors. A violation of GCL cause GCL errors which depend on grid smoothness, grid metrics method and finite difference operators. As a result there are more source terms in spatial discretization errors. The analysis shows that the spatial discretization accuracy on non-sufficiently smooth grids is determined by the discontinuity order of grids and can approach one higher order by following GCL. For sufficiently smooth grids, the spatial discretization accuracy is determined by the order of FDSs and FDSs satisfying the GCL can obtain smaller spatial discretization errors. Numerical tests have been done by the second-order and fourth-order FDSs to verify the theoretical results.

AMS subject classifications: 35L04, 65D25, 65D18, 65M06, 65M15

Key words: Geometric conservation law, finite difference scheme, spatial discretization error, nonsmooth grids, high-order accuracy.

1 Introduction

High-order finite difference schemes (FDSs), which can be constructed easily and have high computational efficiency, are widely used in large eddy simulations (LES) and direct

*Corresponding author. *Email addresses:* mlmao@cardc.cn (M. Mao), hjzhu@skla.cardc.cn (H. Zhu), xgdeng2000@vip.sina.com (X. Deng), ybmin@skla.cardc.cn (Y. Min), hyliu@skla.cardc.cn (H. Liu)

 ©2015 Global-Science Press

https://doi.org/10.4208/cicp.250614.060215a Published online by Cambridge University Press

numerical simulations (DNS) of turbulences and aeroacoustics [1–4]. However, in order to obtain their designed accuracy, FDSs always require sufficiently smooth grids which are very difficult or even impossible to be generated for complex geometries. Complex grids for calculations on practical geometries usually contain nonsmooth features such as slope discontinuities, skewness and stretching, and the impact of these factors on scheme performance is usually significant [5]. Therefore, it is extremely important to study the influence of grid nonsmoothness on spatial accuracy for applications of high-order FDSs to practical engineering problems involving complex geometries.

It has been announced that high-order FDSs can achieve their designed accuracy on sufficiently smooth grids but will degrade their accuracy on non-sufficiently smooth grids. Casper et al. [6] pointed out that a nonsmooth grid will adversely affect the results of finite difference ENO schemes and a sufficiently smooth grid is required to achieve the designed accuracy. Castillo et al. [7] found that the accuracy of fourth-order method degrades gradually as the smoothness of the grid degenerates. Shu [8] also pointed out that the smoothness of meshes must be comparable with the order of accuracy of finite difference WENO schemes in order to obtain a truly high-order result, and the smooth meshes for the fifth-order method mean that at least the fifth derivative of coordinate transformation is continuous. However, the impact of grid smoothness on accuracy of finite difference schemes is usually analyzed numerically but not theoretically.

It was proved that the geometric conservation law (GCL) shall be also satisfied when high-order FDSs are used in the curvilinear coordinates, otherwise some negative effects may appear [9–20], such as violation of free-stream conservation, numerical oscillation. It is true that the GCL is satisfied analytically, but the discrete GCL may be dissatisfied by unsuitable discrete algorithm even on some sufficiently smooth grids, let alone non-sufficiently smooth grids. In recent years, some numerical results showed that satisfying GCL can reduce the requirement on grid smoothness for high-order FDSs, which make it possible to use them to solve problems with complex geometries. In addition, increasing numerical evidences show that satisfying the discrete GCL can improve the time-accuracy of numerical computations and can improve stabilities of these schemes as well (see, e.g., [21–24]). Nonomura et al. [25] showed that the free-stream and vortex preservation properties of WCNS [26–28] is superior to those of the WENO scheme [29], and Deng et al. [30] found the essential reason is that conservative metric method (CMM) can be introduced to ensure WCNS satisfying the GCL. Recently, Nonomura et al. [31] also introduced a technique to make WENO satisfy the GCL and found that with this technique the resolution of vortex is much improved on wavy and random grids. In order to ensure the GCL for high-order finite difference schemes, CMM has been proposed in [30] and a special case of the CMM can be found in Visbal and Gaitonde's numerical technique [5]. Thereafter, symmetrical conservative metric method (SCMM) is derived by analyzing the geometric meaning of metrics and Jacobian [32]. However, the impact of the GCL on spatial accuracy of FDSs has not been analyzed theoretically. For instance, as shown in Refs. [5, 25, 30] correct solutions can be obtained on random grids by FDSs provided that the GCL is satisfied strictly, otherwise, wrong solutions may be yielded if

https://doi.org/10.4208/cicp.250614.060215a Published online by Cambridge University Press

the GCL is not satisfied.

Most of previous work focus on ensuring the GCL for high-order FDSs to obtain better solutions in nonsmooth grids while the reason GCL-FD(FDSs satisfying the GCL) can improve solutions is ignored and not clear up to now. To understand this reason, theoretical and numerical analysis on the accuracy of GCL-FD and NGCL-FD(FDSs which does not satisfy the GCL) are made on nonsmooth grids in the current work. In addition, we denote FDSs with a rth-order accuracy as FDr. Then the rth-order accurate GCL-FD and NGCL-FD are denoted as GCL-FDr and NGCL-FDr, respectively. The main contributions of the work go as follows:

1. Systematic methodology for analyzing numerical errors of finite difference schemes on nonsmooth grids is developed. Our main technique is to use Taylor series expansion based on single-side partial derivatives on discontinuous points.

2. GCL errors and spatial discretization errors are analyzed theoretically. GCL errors are proved to be zero for GCL-FD but be related to grid smoothness and difference operators for NGCL-FD. GCL errors can affect spatial discretization errors. GCL-FD has one order higher spatial accuracy than NGCL-FD for non-sufficiently smooth grids.

3. Numerical tests on GCL errors and spatial discretization errors are made based on grids with different orders of smoothness.

This paper is organized as follows. In Section 2, definitions of grid smoothness and some propositions are presented. In Section 3, GCL errors are analyzed theoretically. In Section 4, spatial discretization errors are analyzed theoretically. In Section 5, numerical tests are made for GCL errors and spatial discretization errors based on grids with different orders of smoothness. Finally, concluding remarks are made in Section 6.

2 Definition of grid smoothness and some propositions

Grid discontinuity will cause some difficulties in analyzing the discrete errors of FDSs theoretically. There are mainly two difficulties: The first is how to describe grid discontinuities mathematically, and the second is how to analyze the influence of grid discontinuities on spatial discretization errors of finite difference operators. In addition, the analysis becomes more complicated when the spatial dimension increases. Take three dimensions for an example, discontinuities may exist in any of the three directions and the Taylor expanding will have many cross-partial derivatives. As a start we consider two dimensional grids and discuss the case that grid coordinates can be written as a smooth function plus another nonsmooth function which can be written as a finite sum of products of one-dimensional functions. Some grids of this kind can be found later in Fig. 1. As for more general grids and three dimensional grids, we like to leave for considering in

https://doi.org/10.4208/cicp.250614.060215a Published online by Cambridge University Press

the future. Moreover, we analyze only the stationary grids in this paper. The grids considered in this paper can be transformed from Cartesian $x-y$ coordinates to curvilinear $\xi-\eta$ coordinates,

$$\begin{cases} x(\xi,\eta)=f(\xi,\eta)+\sum_{m=1}^{M}[\varphi_{m,1}(\xi)\varphi_{m,2}(\eta)], \\ y(\xi,\eta)=g(\xi,\eta)+\sum_{n=1}^{N}[\psi_{n,1}(\xi)\psi_{n,2}(\eta)], \end{cases} \quad \xi\in[0,1],\ \eta\in[0,1]. \tag{2.1}$$

where f and g are sufficiently smooth functions while $\varphi_{m,l}$ and $\psi_{n,l}$ ($l=1,2$, $m=1,2,\cdots,M$, $n=1,2,\cdots,N$) are piecewise-smooth functions. Suppose computational grid has $N_\xi+1$ and $N_\eta+1$ grid points along grid lines $\xi=\xi_i$ and $\eta=\eta_j$, respectively. Coordinates of grid points are $x_{i,j}=x(\xi_i,\eta_j)$ and $y_{i,j}=y(\xi_i,\eta_j)$, where $\xi_i=(i-1)\Delta\xi, \eta_j=(j-1)\Delta\eta, \Delta\xi=1/N_\xi, \Delta\eta=1/N_\eta, i=1,2,\cdots,N_\xi+1$ and $j=1,2,\cdots,N_\eta+1$.

In the following, we give some definitions of grid smoothness and some propositions which are used in Sections 3 and 4 to derive and analyze GCL errors and spatial discretization errors.

Definition 2.1. (Local ξ-continuity) Assume $\left(\frac{\partial^q\phi}{\partial\xi^q}\right)^L_{i,j}$ and $\left(\frac{\partial^q\phi}{\partial\xi^q}\right)^R_{i,j}$ are the qth partial derivatives on the left side and the right side of the ith-point along the grid line $\eta=\eta_j$, if

$$\left(\frac{\partial^q\phi}{\partial\xi^q}\right)^L_{i,j}=\left(\frac{\partial^q\phi}{\partial\xi^q}\right)^R_{i,j} \text{ for } q\le k-1; \quad \left(\frac{\partial^k\phi}{\partial\xi^k}\right)^L_{i,j}\neq\left(\frac{\partial^k\phi}{\partial\xi^k}\right)^R_{i,j},$$

then ϕ is $(k-1)$th-order ξ-continuous at the point (i,j), which is the kth-order ξ-discontinuous point. Here k is called the order of ξ-discontinuity of ϕ.

Definition 2.2. (global ξ-continuity) Suppose ϕ is $n_{i,j}$th-order continuous about ξ at (i,j), and $n=\min\left(n_{1,1},n_{1,2},\cdots,n_{N_\xi+1,N_\eta+1}\right)$. We say that ϕ is nth-order globally ξ-continuous.

Definition 2.3. (C^n grid) If $x(\xi,\eta)$ is n_1th-order globally ξ-continuous and n_2th-order globally η-continuous, and $y(\xi,\eta)$ is n_3th-order globally ξ-continuous and n_4th-order globally η-continuous, we call such a grid is nth-order global continuous grid or C^n grid, where $n=\min\{n_1,n_2,n_3,n_4\}$.

For sufficiently smooth function ϕ, some propositions are presented in the following.

Proposition 2.1. Assume ϕ is sufficiently continuous at ξ_i, and $\phi(\xi)$ can be expanded in Taylor series and the corresponding convergent region is $[-R,R]$. Then, for arbitrary two points ξ_M and ξ_N in this convergent region, we have

$$\sum_{q=1}^{\infty}\frac{(\xi_M-\xi_i)^q}{q!}\left(\frac{\partial^q\phi}{\partial\xi^q}\right)_i+\sum_{q=1}^{\infty}\frac{(\xi_N-\xi_M)^q}{q!}\left(\frac{\partial^q\phi}{\partial\xi^q}\right)_M=\sum_{q=1}^{\infty}\frac{(\xi_N-\xi_i)^q}{q!}\left(\frac{\partial^q\phi}{\partial\xi^q}\right)_i. \tag{2.2}$$

https://doi.org/10.4208/cicp.250614.060215a Published online by Cambridge University Press

This proposition can be easily proved by using the following Taylor series expansion

$$\left(\frac{\partial^q \phi}{\partial \xi^q}\right)_M = \left(\frac{\partial^q \phi}{\partial \xi^q}\right)_i + \sum_{r=1}^{\infty}\left[\frac{(\xi_M-\xi_i)^r}{r!}\left(\frac{\partial^{q+r}\phi}{\partial \xi^{q+r}}\right)_i\right]$$

and Binomial Theorem.

Suppose ϕ is discontinuous at the point (i,j), the following Taylor series expansion based on single-side partial derivatives can be obtained,

$$\phi_{i+l,j}-\phi_{i,j}=\begin{cases}\displaystyle\sum_{q=1}^{\infty} l^q \frac{(\Delta\xi)^q}{q!}\left(\frac{\partial^q\phi}{\partial^q\xi}\right)_{i,j}^{R}, & l>0,\\ \displaystyle\sum_{q=1}^{\infty} l^q \frac{(\Delta\xi)^q}{q!}\left(\frac{\partial^q\phi}{\partial^q\xi}\right)_{i,j}^{L}, & l<0.\end{cases} \tag{2.3}$$

Proposition 2.2. Suppose ϕ is continuous at the point (i,j) but discontinuous at point $i_A=i+i_D$ $(i_D\neq 0)$ which is between i and $i+l$, then we have

$$\phi_{i+l,j}-\phi_{i,j}=\sum_{q=1}^{\infty} l^q \frac{(\Delta\xi)^q}{q!}\left(\frac{\partial^q\phi}{\partial^q\xi}\right)_{i,j}+\text{sign}(i_D)\sum_{q=1}^{\infty}(l-i_D)^q\frac{(\Delta\xi)^q}{q!}\left(\frac{\partial^q\phi}{\partial^q\xi}\right)_{i_A,j}^{R-L}, \tag{2.4}$$

where $(\cdot)^{R-L}$ is defined as the difference between the right side and the left side values at the same point, i.e., $(\cdot)^{R-L}=(\cdot)^R-(\cdot)^L$.

Proof. For $i_D>0$, we notice that

$$\begin{aligned}\phi_{i+l,j}-\phi_{i,j}&=\phi_{i+l,j}-\phi_{i_A,j}+\phi_{i_A,j}-\phi_{i,j}\\ &=\sum_{q=1}^{\infty}(l-i_D)^q\frac{(\Delta\xi)^q}{q!}\left(\frac{\partial^q\phi}{\partial^q\xi}\right)_{i_A,j}^{R}+\sum_{q=1}^{\infty}(i_D)^q\frac{(\Delta\xi)^q}{q!}\left(\frac{\partial^q\phi}{\partial^q\xi}\right)_{i,j}\\ &=\sum_{q=1}^{\infty}(l-i_D)^q\frac{(\Delta\xi)^q}{q!}\left(\frac{\partial^q\phi}{\partial^q\xi}\right)_{i_A,j}^{R-L}+\sum_{q=1}^{\infty}(i_D)^q\frac{(\Delta\xi)^q}{q!}\left(\frac{\partial^q\phi}{\partial^q\xi}\right)_{i,j}\\ &\quad+\sum_{q=1}^{\infty}(l-i_D)^q\frac{(\Delta\xi)^q}{q!}\left(\frac{\partial^q\phi}{\partial^q\xi}\right)_{i_A,j}^{L}.\end{aligned} \tag{2.5}$$

In addition, from Proposition 2.1 we have

$$\sum_{q=1}^{\infty}(i_D)^q\frac{(\Delta\xi)^q}{q!}\left(\frac{\partial^q\phi}{\partial^q\xi}\right)_{i,j}+\sum_{q=1}^{\infty}(l-i_D)^q\frac{(\Delta\xi)^q}{q!}\left(\frac{\partial^q\phi}{\partial^q\xi}\right)_{i_A,j}^{L}=\sum_{q=1}^{\infty}l^q\frac{(\Delta\xi)^q}{q!}\left(\frac{\partial^q\phi}{\partial^q\xi}\right)_{i,j}. \tag{2.6}$$

Therefore, (2.4) can be obtained by combining (2.5) and (2.6). The result for $i_D<0$ can be obtained by a similar deductive procedure. □

https://doi.org/10.4208/cicp.250614.060215a Published online by Cambridge University Press

For the difference operator of the first partial derivative $\frac{\partial\phi}{\partial\xi}$,

$$\delta^{\xi}\phi_{i,j}=\frac{1}{\Delta\xi}\sum_{m=-M_1}^{M_2}b_m(\phi_{i+m,j}-\phi_{i,j}), \tag{2.7}$$

if the operator has rth-order accuracy, the relation of $\{b_m\}$ can be easily obtained by taking Taylor series expansion of $\phi_{i+m,j}$ at $\phi_{i,j}$

$$\sum_{m=-M_1}^{M_2}mb_m=1,\qquad \sum_{m=-M_1}^{M_2}m^qb_m=0,\ 2\le q\le r\ \text{ or }\ q=0. \tag{2.8}$$

Since the operator has rth-order accuracy, i.e.

$$\delta^{\xi}\phi_{i,j}=\left(\frac{\partial\phi}{\partial\xi}\right)_{i,j}+\mathcal{O}((\Delta\xi)^r). \tag{2.9}$$

Then, we consider the discretization errors of the difference operator $\delta^{\xi}\phi$ of the first derivative ϕ_{ξ}.

Proposition 2.3. Suppose ϕ is kth-order ξ-partial discontinuous at point (i_A,j) along the grid line $\eta=\eta_j$, and is continuous on the both sides of this point. Set $i_A=i_D+i$. We have for $i_D>0$

$$\begin{aligned}\delta^{\xi}\phi_{i,j}=&\sum_{m=-M_1^{\xi}}^{M_2^{\xi}}b_m^{\xi}\sum_{q=1}^{\infty}\frac{m^q(\Delta\xi)^{q-1}}{q!}\left(\frac{\partial^q\phi}{\partial\xi^q}\right)_{i,j}\\&+\sum_{m=i_D+1}^{M_2^{\xi}}b_m^{\xi}\sum_{q=k}^{\infty}\frac{(m-i_D)^q(\Delta\xi)^{q-1}}{q!}\left(\frac{\partial^q\phi}{\partial\xi^q}\right)_{i_A,j}^{R-L};\end{aligned} \tag{2.10a}$$

for $i_D<0$,

$$\begin{aligned}\delta^{\xi}(\phi)_{i,j}=&\sum_{m=-M_1^{\xi}}^{M_2^{\xi}}b_m^{\xi}\sum_{q=1}^{\infty}\frac{m^q(\Delta\xi)^{q-1}}{q!}\left(\frac{\partial^q\phi}{\partial\xi^q}\right)_{i,j}\\&-\sum_{m=-M_1^{\xi}}^{i_D}b_m^{\xi}\sum_{q=k}^{\infty}\frac{(m-i_D)^q(\Delta\xi)^{q-1}}{q!}\left(\frac{\partial^q\phi}{\partial\xi^q}\right)_{i_A,j}^{R-L};\end{aligned} \tag{2.10b}$$

and for $i_D=0$,

$$\begin{aligned}\delta^{\xi}(\phi)_{i,j}=&\sum_{m=-M_1^{\xi}}^{i_D}b_m^{\xi}\sum_{q=1}^{\infty}\frac{(m-i_D)^q(\Delta\xi)^{q-1}}{q!}\left(\frac{\partial^q\phi}{\partial\xi^q}\right)_{i_A,j}^{L}\\&+\sum_{m=i_D+1}^{M_2^{\xi}}b_m^{\xi}\sum_{q=1}^{\infty}\frac{(m-i_D)^q(\Delta\xi)^{q-1}}{q!}\left(\frac{\partial^q\phi}{\partial\xi^q}\right)_{i_A,j}^{R}.\end{aligned} \tag{2.10c}$$

https://doi.org/10.4208/cicp.250614.060215a Published online by Cambridge University Press

Here the superscript in b_m^ξ denotes the coefficients of the partial derivatives in ξ direction. Proposition 2.3 can be easily proved based on single-side Taylor expanding (2.3) and Proposition 2.2.

For convenient and without loss of generality, hereinafter we assume that the computational point (i,j) locates at the left side of the discontinuous point (i_A,j) and satisfies that $i_A=i+i_D$ with $i_D>0$.

For rth-order difference operator,

$$\sum_{m=-M_1^\xi}^{M_2^\xi} b_m^\xi \sum_{q=1}^{\infty} \frac{m^q(\Delta\xi)^{q-1}}{q!}\left(\frac{\partial^q\phi}{\partial\xi^q}\right)_{i,j} = \frac{\partial\phi}{\partial\xi}+\mathcal{O}((\Delta\xi)^r). \tag{2.11}$$

Inserting (2.11) into (2.10), we can get

$$\delta^\xi\phi_{i,j} = \left(\frac{\partial\phi}{\partial\xi}\right)_{i,j} + \sum_{m=i_D+1}^{M_2^\xi} b_m^\xi \sum_{q=k}^{\infty} \frac{(m-i_D)^q(\Delta\xi)^{q-1}}{q!}\left(\frac{\partial^q\phi}{\partial\xi^q}\right)_{i_A,j}^{R-L} + \mathcal{O}((\Delta\xi)^r). \tag{2.12}$$

Proposition 2.4. If u is an infinitely differentiable function about x and y, and i_A is the kth-order ξ-discontinuous point of x,y. Then, the following relation holds

$$\left(\frac{\partial^k u}{\partial\xi^k}\right)_{i_A,j}^{R-L} = \left(\frac{\partial u}{\partial y}\right)_{i_A,j}\left(\frac{\partial^k y}{\partial\xi^k}\right)_{i_A,j}^{R-L} + \left(\frac{\partial u}{\partial x}\right)_{i_A,j}\left(\frac{\partial^k x}{\partial\xi^k}\right)_{i_A,j}^{R-L}. \tag{2.13}$$

Proof. Firstly, expanding $\frac{\partial^k u}{\partial\xi^k}$ by chain rule, we notice that the terms which contain the kth partial derivatives of x and y about ξ are $\frac{\partial u}{\partial x}\frac{\partial^k x}{\partial\xi^k}$ and $\frac{\partial u}{\partial y}\frac{\partial^k y}{\partial\xi^k}$. In addition, according to the kth partial derivative discontinuity in Definition 2.1, we have

$$\left(\frac{\partial^q x}{\partial\xi^q}\right)_{i_A,j}^{R} = \left(\frac{\partial^q x}{\partial\xi^q}\right)_{i_A,j}^{L}, \quad \left(\frac{\partial^q y}{\partial\xi^q}\right)_{i_A,j}^{R} = \left(\frac{\partial^q y}{\partial\xi^q}\right)_{i_A,j}^{L}, \quad q\le k-1,$$
$$\left(\frac{\partial^k x}{\partial\xi^k}\right)_{i_A,j}^{R} \neq \left(\frac{\partial^k x}{\partial\xi^k}\right)_{i_A,j}^{L}, \quad \left(\frac{\partial^k y}{\partial\xi^k}\right)_{i_A,j}^{R} \neq \left(\frac{\partial^k y}{\partial\xi^k}\right)_{i_A,j}^{L}.$$

Therefore, (2.13) is obtained immediately. □

If u is an infinitely differentiable function about y, and i_A is the kth-order ξ-discontinuous point of y, then the relation (2.13) reduces to

$$\left(\frac{\partial^k u}{\partial\xi^k}\right)_{i_A,j}^{R-L} = \left(\frac{\partial u}{\partial y}\right)_{i_A,j}\left(\frac{\partial^k y}{\partial\xi^k}\right)_{i_A,j}^{R-L}.$$

Remark 2.1. Under the transformation in (2.1), $\frac{\partial^p\phi}{\partial\eta^p}$ $(p\ge 1)$ have the same order of ξ-discontinuity as ϕ, and $\frac{\partial^q\phi}{\partial\xi^q}$ $(q\ge 1)$ have the same order of η-discontinuity as ϕ. Here ϕ is the coordinate x or y.

https://doi.org/10.4208/cicp.250614.060215a Published online by Cambridge University Press

3 GCL discretization errors

If a FDS does not satisfy the GCL, the GCL errors may cause many unpleasant problems like numerical oscillations and free-stream violation. The GCL errors of GCL-FD and NGCL-FD are analyzed in this section.

Two-dimensional transformation from Cartesian coordinates $x-y$ to curvilinear coordinates $\xi-\eta$ shall satisfy the following differential GCL

$$I_x=\frac{\partial\widehat{\xi}_x}{\partial\xi}+\frac{\partial\widehat{\eta}_x}{\partial\eta}=0,\quad I_y=\frac{\partial\widehat{\xi}_y}{\partial\xi}+\frac{\partial\widehat{\eta}_y}{\partial\eta}=0, \tag{3.1}$$

where

$$\begin{cases}\widehat{\xi}_x=J\xi_x=\ \ y_\eta,\\ \widehat{\xi}_y=J\xi_y=-x_\eta,\end{cases}\quad\begin{cases}\widehat{\eta}_x=J\eta_x=-y_\xi,\\ \widehat{\eta}_y=J\eta_y=\ \ x_\xi.\end{cases} \tag{3.2}$$

Here the grid metrics are

$$J=\left|\frac{\partial(x,y)}{\partial(\xi,\eta)}\right|=x_\xi y_\eta-x_\eta y_\xi. \tag{3.3}$$

According to (3.2), the discrete form of the GCL (3.1) can be written as

$$\widetilde{I}_x=\delta_1^\xi(\delta_2^\eta y)-\delta_1^\eta(\delta_2^\xi y),\quad \widetilde{I}_y=-\delta_1^\xi(\delta_2^\eta x)+\delta_1^\eta(\delta_2^\xi x), \tag{3.4}$$

where δ_1 and δ_2 are called the first and second difference operator of (3.1). Here $\widetilde{(\cdot)}$ represents the discrete form of $(\cdot)$. It is worth noting that δ_2 is used to compute the grid metrics while δ_1 is used to compute flux derivatives. In curvilinear coordinate, since flux derivatives contain grid metrics, δ_1 also operates the metrics. A general form of δ_1 and δ_2 can be written as,

$$\delta_1^\xi\psi_i=\frac{1}{\Delta\xi}\sum_{l=-L_1^\xi}^{L_2^\xi}a_l^\xi(\psi_{i+l}-\psi_i),\quad \delta_2^\xi\phi_i=\frac{1}{\Delta\xi}\sum_{m=-M_1^\xi}^{M_2^\xi}b_m^\xi(\phi_{i+m}-\phi_i), \tag{3.5a}$$

$$\delta_1^\eta\psi_j=\frac{1}{\Delta\eta}\sum_{l=-L_1^\eta}^{L_2^\eta}a_l^\eta(\psi_{j+l}-\psi_j),\quad \delta_2^\eta\phi_j=\frac{1}{\Delta\eta}\sum_{m=-M_1^\eta}^{M_2^\eta}b_m^\eta(\phi_{j+m}-\phi_j). \tag{3.5b}$$

The discrete GCL errors of GCL-FD and NGCL-FD are given in the following theorem.

Theorem 3.1. *Assume the grid is kth-order discontinuous, and x,y are sufficiently smooth in η direction but kth-order ξ-discontinuous. Suppose the finite difference operator has rth-order accuracy. Then, we have*

(i) *For GCL-FD, which satisfies the CMM condition as $\delta_1^\xi=\delta_2^\xi$ and $\delta_1^\eta=\delta_2^\eta$, then $\widetilde{I}_x=0$ and $\widetilde{I}_y=0$.*

https://doi.org/10.4208/cicp.250614.060215a Published online by Cambridge University Press

(ii) *For NGCL-FD, which does not satisfy the above CMM condition, the GCL errors are*

$$(\widetilde{I}_x)_{i,j}=(\widetilde{I}_y)_{i,j}=\mathcal{O}((\Delta\xi)^{\min\{r,k-1\}},(\Delta\eta)^r). \tag{3.6}$$

Proof. Using the results (2.10) in Proposition 2.3, we obtain

$$\begin{aligned}
(\widetilde{I}_x)_{i,j}=&\delta_1^\xi(\delta_2^\eta y_{i,j})-\delta_1^\eta(\delta_2^\xi y_{i,j})\\
=&\frac{1}{\Delta\xi}\sum_{l=-L_1^\xi}^{L_2^\xi}a_l^\xi(\delta_2^\eta y_{i+l,j}-\delta_2^\eta y_{i,j})-\frac{1}{\Delta\eta}\sum_{l=-L_1^\eta}^{L_2^\eta}a_l^\eta(\delta_2^\xi y_{i,j+l}-\delta_2^\xi y_{i,j})\\
=&\frac{1}{\Delta\xi}\sum_{l=-L_1^\xi}^{L_2^\xi}a_l^\xi\sum_{m=-M_1^\eta}^{M_2^\eta}b_m^\eta\sum_{p=1}^{\infty}\frac{m^p(\Delta\eta)^{p-1}}{p!}\left[\left(\frac{\partial^p y}{\partial\eta^p}\right)_{i+l,j}-\left(\frac{\partial^p y}{\partial\eta^p}\right)_{i,j}\right]\\
&-\frac{1}{\Delta\eta}\sum_{l=-L_1^\eta}^{L_2^\eta}a_l^\eta\sum_{m=-M_1^\xi}^{M_2^\xi}b_m^\xi\sum_{q=1}^{\infty}\frac{m^q(\Delta\xi)^{q-1}}{q!}\left[\left(\frac{\partial^q y}{\partial\xi^q}\right)_{i,j+l}-\left(\frac{\partial^q y}{\partial\xi^q}\right)_{i,j}\right]\\
&-\frac{1}{\Delta\eta}\sum_{l=-L_1^\eta}^{L_2^\eta}a_l^\eta\sum_{m=i_D+1}^{M_2^\xi}b_m^\xi\sum_{q=1}^{\infty}\frac{(m-i_D)^q(\Delta\xi)^{q-1}}{q!}\times\left[\left(\frac{\partial^q y}{\partial\xi^q}\right)_{i_A,j+l}^{R-L}-\left(\frac{\partial^q y}{\partial\xi^q}\right)_{i_A,j}^{R-L}\right].
\end{aligned}\tag{3.7}$$

Then, by using Taylor series expansion in η direction and Proposition 2.3 once again, we can obtain

$$(\widetilde{I}_x)_{i,j}=\widetilde{I}_{sm}+\widetilde{I}_{nsm}, \tag{3.8}$$

where

$$\begin{aligned}
\widetilde{I}_{sm}=&\sum_{p=1}^{\infty}\sum_{q=1}^{\infty}\frac{(\Delta\eta)^{p-1}(\Delta\xi)^{q-1}}{p!q!}\left(\frac{\partial^{p+q}y}{\partial\eta^p\partial\xi^q}\right)_{i,j}\\
&\times\left(\sum_{l=-L_1^\xi}^{L_2^\xi}a_l^\xi l^q\sum_{m=-M_1^\eta}^{M_2^\eta}b_m^\eta m^p-\sum_{l=-L_1^\eta}^{L_2^\eta}a_l^\eta l^p\sum_{m=-M_1^\xi}^{M_2^\xi}b_m^\xi m^q\right),\\
\widetilde{I}_{nsm}=&\sum_{p=1}^{\infty}\sum_{q=1}^{\infty}\frac{(\Delta\xi)^{q-1}}{q!}\frac{(\Delta\eta)^{p-1}}{p!}\left(\frac{\partial^{p+q}y}{\partial\xi^q\partial\eta^p}\right)_{i_A,j}^{R-L}\\
&\times\left(\sum_{l=i_D+1}^{L_2^\xi}a_l^\xi(l-i_D)^q\sum_{m=-M_1^\eta}^{M_2^\eta}b_m^\eta m^p-\sum_{l=-L_1^\eta}^{L_2^\eta}a_l^\eta l^p\sum_{m=i_D+1}^{M_2^\xi}b_m^\xi(m-i_D)^q\right).
\end{aligned}$$

(i) Since $\delta_1^\xi=\delta_2^\xi$ and $\delta_1^\eta=\delta_2^\eta$, both of $\widetilde{I}_{sm}$ and $\widetilde{I}_{nsm}$ are equal to zero. Therefore, we have $\widetilde{I}_x=0$ for GCL-FD no matter the grid is smooth or not.

(ii) For NGCL-FD, based on the coefficient relations (2.8) and note that the order of discontinuity of $\frac{\partial x}{\partial\eta}$ and $\frac{\partial y}{\partial\eta}$ are the same with x and y correspondingly in ξ direction, the

https://doi.org/10.4208/cicp.250614.060215a Published online by Cambridge University Press

main error of $\widetilde{I}_{sm}$ and $\widetilde{I}_{nsm}$ becomes

$$\left(\sum_{m=-M_1^\eta}^{M_2^\eta} b_m^\eta m^{r+1} - \sum_{l=-L_1^\eta}^{L_2^\eta} a_l^\eta l^{r+1}\right) \frac{(\Delta\eta)^r}{(r+1)!} \left(\frac{\partial^{r+2} y}{\partial \eta^{r+1} \partial \xi}\right)_{i,j}$$
$$+ \left(\sum_{l=-L_1^\xi}^{L_2^\xi} a_l^\xi l^{r+1} - \sum_{m=-M_1^\xi}^{M_2^\xi} b_m^\xi m^{r+1}\right) \frac{(\Delta\xi)^r}{(r+1)!} \left(\frac{\partial^{r+2} y}{\partial \xi^{r+1} \partial \eta}\right)_{i,j} = \mathcal{O}((\Delta\xi)^r, (\Delta\eta)^r),$$

and

$$\left(\sum_{l=i_D+1}^{L_2^\xi} a_l^\xi (l-i_D)^k - \sum_{m=i_D+1}^{M_2^\xi} b_m^\xi (m-i_D)^k\right) \frac{(\Delta\xi)^{k-1}}{k!} \left(\frac{\partial^{1+k} y}{\partial \xi^k \partial \eta}\right)_{i_A,j}^{R-L} = \mathcal{O}((\Delta\xi)^{k-1}).$$

Thus, the GCL error is

$$(\widetilde{I}_x)_{i,j} = \mathcal{O}\left((\Delta\xi)^{\min\{r,k-1\}}, (\Delta\eta)^r\right). \tag{3.9}$$

By similar deductive procedure, the GCL error of I_y can be obtained by replacing y in (3.9) with x. Thus, we have $\widetilde{I}_y = 0$ for GCL-FD and $\widetilde{I}_y = \mathcal{O}\left((\Delta\xi)^{\min\{r,k-1\}}, (\Delta\eta)^r\right)$ for NGCL-FD. □

Then it is evident that the convergence order of the GCL errors for NGCL-FDr is $\min\{k-1, r\}$. From (3.6), we note that if the grid is sufficiently smooth ($k \geq r+1$), the convergence order of the GCL errors is equal to the spatial accuracy order of the finite difference operator.

Proposition 3.1. For a C^k grid (defined in 2.3) where x, y have discontinuities in both ξ and η direction, the GCL errors of NGCL-FDr are determined by the lowest order of discontinuities and the convergence order is also $\min\{k-1, r\}$.

This proposition can be proved by using Taylor series expansion and considering both the ξ-partial discontinuity and the η-partial discontinuity simultaneously. Details of the proof process are omitted in this paper to save space.

In addition, the relation between L_m norm errors and L_∞ norm errors is also derived. For sufficiently smooth grids, the convergence rates of L_m errors are the same as L_∞ errors, while for nonsmooth grids which have a finite number of discontinuities, the relation becomes $Order(L_m) = Order(L_\infty) + 1/m$. The derivation process of the relation is not detailed here.

4 Spatial discretization errors

In this section, we analyze spatial discretization errors of GCL-FD and NGCL-FD based on nonsmooth grids.

https://doi.org/10.4208/cicp.250614.060215a Published online by Cambridge University Press

Consider the following conservation law

$$\frac{\partial u}{\partial t}+\frac{\partial E(u)}{\partial x}+\frac{\partial F(u)}{\partial y}=0. \tag{4.1}$$

By using curvilinear coordinates transformation (2.1), (4.1) becomes

$$\frac{\partial Ju}{\partial t}+\frac{\partial(E\widehat{\xi}_x+F\widehat{\xi}_y)}{\partial\xi}+\frac{\partial(E\widehat{\eta}_x+F\widehat{\eta}_y)}{\partial\eta}=0. \tag{4.2}$$

Substituting (3.2) into (4.2), we obtain

$$\frac{\partial u}{\partial t}+\frac{A}{J}=0, \tag{4.3}$$

where A is the flux part

$$A=\left[\frac{\partial(Ey_\eta-Fx_\eta)}{\partial\xi}+\frac{\partial(Fx_\xi-Ey_\xi)}{\partial\eta}\right]. \tag{4.4}$$

We split the flux part A into two parts, i.e.,

$$A=A_E+A_F \tag{4.5}$$

with the E-flux part

$$A_E=(Ey_\eta)_\xi-(Ey_\xi)_\eta \tag{4.6}$$

and the F-flux part

$$A_F=-\left((Fx_\eta)_\xi-(Fx_\xi)_\eta\right). \tag{4.7}$$

In the following, we will analyze the discretization errors of A and J, respectively.

4.1 Discretization errors of the flux part

Now we analyze the discretization errors of A. Firstly, the errors of A_E and A_F will be analyzed separately. Then, the discretization errors of A will be obtained by adding the errors of A_E and A_F.

4.1.1 Discretization errors of the E-flux part

By using the operators in (3.5), the discretization form of the E-flux part (4.6) reads

$$\left(\widetilde{A_E}\right)_{i,j}=\delta_1^\xi(E\delta_2^\eta y)_{i,j}-\delta_1^\eta(E\delta_2^\xi y)_{i,j}=(A_E)_{i,j}+(e_{A_E})_{i,j}. \tag{4.8}$$

https://doi.org/10.4208/cicp.250614.060215a Published online by Cambridge University Press

At the end, the discretization errors of A_E can be evaluated as (see Appendix for details)

$$(e_{A_E})_{i,j}=e^E_{GCL}+e^E_{nsm1}+e^E_{nsm2}+\mathcal{O}\left((\Delta\xi)^{\min\{r,k\}},(\Delta\eta)^r\right), \tag{4.9}$$

where

$$e^E_{GCL}=(\widetilde{I}_x)_{i,j}E_{i,j},$$

$$e^E_{nsm1}=\left(\frac{\partial E}{\partial y}\right)_{i,j}\left(\frac{\partial y}{\partial \eta}\right)_{i,j}\left(\frac{\partial^k y}{\partial \xi^k}\right)^{R-L}_{i_A,j}\frac{(\Delta\xi)^{k-1}}{k!}\left[\sum_{l=i_D+1}^{L_2^\xi}a_l^\xi(l-i_D)^k-\sum_{m=i_D+1}^{M_2^\xi}b_m^\xi(m-i_D)^k\right],$$

$$e^E_{nsm2}=\left(\frac{\partial E}{\partial x}\right)_{i,j}\left(\frac{\partial y}{\partial \eta}\right)_{i,j}\left(\frac{\partial^k x}{\partial \xi^k}\right)^{R-L}_{i_A,j}\frac{(\Delta\xi)^{k-1}}{k!}\sum_{l=i_D+1}^{L_2^\xi}a_l^\xi(l-i_D)^k$$
$$-\left(\frac{\partial E}{\partial x}\right)_{i,j}\left(\frac{\partial x}{\partial \eta}\right)_{i,j}\left(\frac{\partial^k y}{\partial \xi^k}\right)^{R-L}_{i_A,j}\frac{(\Delta\xi)^{k-1}}{k!}\sum_{m=i_D+1}^{M_2^\xi}b_m^\xi(m-i_D)^k.$$

If a GCL-FD is applied to the flux part (4.4), which means that the difference operators satisfy the conditions of $\delta_1^\xi=\delta_2^\xi$ and $\delta_1^\eta=\delta_2^\eta$. Then, according to Theorem 3.1(i), the GCL error is equal to zero, thus

$$e^E_{GCL}=0.$$

Furthermore, since $\delta_1^\xi=\delta_2^\xi$, we have

$$\sum_{l=i_D+1}^{L_2^\xi}a_l^\xi(l-i_D)^k-\sum_{m=i_D+1}^{M_2^\xi}b_m^\xi(m-i_D)^k=0. \tag{4.10}$$

Thus $e^E_{nsm1}=0$. Moreover, from (4.10), e^E_{nsm2} can be simplified as

$$e^E_{nsm2}=\frac{(\Delta\xi)^{k-1}}{k!}\left(\frac{\partial E}{\partial x}\right)_{i,j}g_{i,j}\sum_{l=i_D+1}^{L_2^\xi}a_l^\xi(l-i_D)^k,$$

where

$$g_{i,j}=\left(\frac{\partial y}{\partial \eta}\right)_{i,j}\left(\frac{\partial^k x}{\partial \xi^k}\right)^{R-L}_{i_A,j}-\left(\frac{\partial x}{\partial \eta}\right)_{i,j}\left(\frac{\partial^k y}{\partial \xi^k}\right)^{R-L}_{i_A,j}. \tag{4.11}$$

Therefore, e_{A_E} becomes

$$(e_{A_E})_{i,j}=\mathcal{O}\left((\Delta\xi)^{\min\{r,k\}},(\Delta\eta)^r\right)+\frac{(\Delta\xi)^{k-1}}{k!}\left(\frac{\partial E}{\partial x}\right)_{i,j}g_{i,j}\sum_{l=i_D+1}^{L_2^\xi}a_l^\xi(l-i_D)^k.$$

From (4.9) we can see that, for sufficiently smooth grid ($k\geq r+1$), the E flux part of GCL-FD does not have the error term e^E_{GCL}, which is of $\mathcal{O}((\Delta\xi)^r,(\Delta\eta)^r)$ according to Theorem 3.1(ii). Therefore, satisfying GCL may help to reduce numerical errors even for sufficiently smooth grid.

https://doi.org/10.4208/cicp.250614.060215a Published online by Cambridge University Press

4.1.2 Discretization errors of the F-flux part

In a similar deductive procedure, the discretization errors of the F-flux part can be obtained,

$$(e_{A_F})_{i,j}=e^F_{GCL}+e^F_{nsm1}+e^F_{nsm2}+\mathcal{O}\left((\Delta\xi)^{\min\{r,k\}},(\Delta\eta)^r\right), \tag{4.12}$$

where

$$e^F_{GCL}=(\widetilde{I}_y)_{i,j}F_{i,j},$$

$$e^F_{nsm1}=-\frac{(\Delta\xi)^{k-1}}{k!}\left[\sum_{l=i_D+1}^{L_2^\xi}a_l^\xi(l-i_D)^k-\sum_{m=i_D+1}^{M_2^\xi}b_m^\xi(m-i_D)^k\right]\left(\frac{\partial F}{\partial x}\right)_{i,j}\left(\frac{\partial x}{\partial\eta}\right)_{i,j}\left(\frac{\partial^k x}{\partial\xi^k}\right)^{R-L}_{i_A,j},$$

$$e^F_{nsm2}=-\frac{(\Delta\xi)^{k-1}}{k!}\sum_{l=i_D+1}^{L_2^\xi}a_l^\xi(l-i_D)^k\left(\frac{\partial F}{\partial y}\right)_{i,j}\left(\frac{\partial x}{\partial\eta}\right)_{i,j}\left(\frac{\partial^k y}{\partial\xi^k}\right)^{R-L}_{i_A,j}$$
$$+\frac{(\Delta\xi)^{k-1}}{k!}\sum_{m=i_D+1}^{M_2^\xi}b_m^\xi(m-i_D)^k\left(\frac{\partial F}{\partial y}\right)_{i,j}\left(\frac{\partial y}{\partial\eta}\right)_{i,j}\left(\frac{\partial^k x}{\partial\xi^k}\right)^{R-L}_{i_A,j}.$$

If GCL-FD is applied to the flux part (4.4), namely $\delta_1^\xi=\delta_2^\xi$ and $\delta_1^\eta=\delta_2^\eta$, we have

$$(e_{A_F})_{i,j}=\mathcal{O}\left((\Delta\xi)^{\min\{r,k\}},(\Delta\eta)^r\right)+\frac{(\Delta\xi)^{k-1}}{k!}\left(\frac{\partial F}{\partial y}\right)_{i,j}g_{i,j}\sum_{l=i_D+1}^{L_2^\xi}a_l^\xi(l-i_D)^k.$$

For sufficiently smooth grid ($k\geq r+1$), the F-flux part of GCL-FD does not have the error term e^F_{GCL}, which is of $\mathcal{O}((\Delta\xi)^r,(\Delta\eta)^r)$.

4.1.3 Discretization errors of the flux part

The discretization errors of A can be obtained by adding the errors of A_E and A_F, i.e.,

$$(e_A)_{i,j}=(e_{A_E})_{i,j}+(e_{A_F})_{i,j}, \tag{4.13}$$

where $(e_{A_E})_{i,j}$ and $(e_{A_F})_{i,j}$ are given in (4.9) and (4.12), respectively.

If $\delta_1^\xi=\delta_2^\xi$, then we have

$$(e_A)_{i,j}=\mathcal{O}\left((\Delta\xi)^{\min\{r,k\}},(\Delta\eta)^r\right)$$
$$+\frac{(\Delta\xi)^{k-1}}{k!}\left(\left(\frac{\partial E}{\partial x}\right)_{i,j}+\left(\frac{\partial F}{\partial y}\right)_{i,j}\right)g_{i,j}\sum_{l=i_D+1}^{L_2^\xi}a_l^\xi(l-i_D)^k. \tag{4.14}$$

For sufficiently smooth grid ($k\geq r+1$), the flux part of GCL-FD does not have the error term $e^E_{GCL}+e^F_{GCL}$, which is of $\mathcal{O}((\Delta\xi)^r,(\Delta\eta)^r)$.

https://doi.org/10.4208/cicp.250614.060215a Published online by Cambridge University Press

We compare the error of NGCL-FD (4.13) with the error of GCL-FD (4.14). For unsteady problem $\left(\frac{\partial E}{\partial x}\right)_{i,j}+\left(\frac{\partial F}{\partial y}\right)_{i,j}\neq 0$, $(e_A)_{i,j}$ is of $\mathcal{O}\left((\Delta\xi)^{\min\{r,k-1\}},(\Delta\eta)^r\right)$ for both NGCL-FD and GCL-FD, but the latter one has less error terms. For steady problem we have

$$(e_A)_{i,j}=\begin{cases}\mathcal{O}\left((\Delta\xi)^{\min\{r,k-1\}},(\Delta\eta)^r\right), & \text{for NGCL}-\text{FD},\\ \mathcal{O}\left((\Delta\xi)^{\min\{r,k\}},(\Delta\eta)^r\right), & \text{for GCL}-\text{FD}.\end{cases} \tag{4.15}$$

4.2 Discretization errors of Jacobian

The Jacobian J defined in (3.3) has two basic equivalent conservation forms,

$$J_0=(xy_\eta)_\xi-(xy_\xi)_\eta,\quad J_1=(yx_\xi)_\eta-(yx_\eta)_\xi.$$

In fact, we have the following general form of the Jacobian,

$$J_a=(1-a)J_0+aJ_1, \tag{4.16}$$

where $0\leq a\leq 1$. The discretization form of J_0 is

$$\left(\widetilde{J_0}\right)_{i,j}=\delta_1^\xi(x\delta_2^\eta y)_{i,j}-\delta_1^\eta(x\delta_2^\xi y)_{i,j}=(J_0)_{i,j}+(e_{J_0})_{i,j}.$$

Replacing E in (4.9) with x and noticing that $\frac{\partial y}{\partial x}=0$, $\frac{\partial x}{\partial x}=1$, $\frac{\partial x}{\partial y}=0$ and $\frac{\partial y}{\partial y}=1$, we obtain

$$\begin{aligned}(e_{J_0})_{i,j}=&(\widetilde{I}_x)_{i,j}x_{i,j}+\mathcal{O}\left((\Delta\xi)^{\min\{r,k\}},(\Delta\eta)^r\right)\\&+\frac{(\Delta\xi)^{k-1}}{k!}\sum_{l=i_D+1}^{L_2^\xi}a_l^\xi(l-i_D)^k\left(\frac{\partial y}{\partial\eta}\right)_{i,j}\left(\frac{\partial^k x}{\partial\xi^k}\right)_{i_A,j}^{R-L}\\&-\frac{(\Delta\xi)^{k-1}}{k!}\sum_{m=i_D+1}^{M_2^\xi}b_m^\xi(m-i_D)^k\left(\frac{\partial x}{\partial\eta}\right)_{i,j}\left(\frac{\partial^k y}{\partial\xi^k}\right)_{i_A,j}^{R-L}.\end{aligned} \tag{4.17}$$

And the discretization form of J_1 is

$$\widetilde{J_1}=\delta_1^\eta(y\delta_2^\xi x)-\delta_1^\xi(y\delta_2^\eta x)=(J_1)_{i,j}+(e_{J_1})_{i,j}.$$

Similarly, e_{J_1} can be obtained by replacing F in (4.12) with y,

$$\begin{aligned}(e_{J_1})_{i,j}=-\Bigg\{&-(\widetilde{I}_y)_{i,j}y_{i,j}+\mathcal{O}\left((\Delta\xi)^{\min\{r,k\}},(\Delta\eta)^r\right)\\&+\frac{(\Delta\xi)^{k-1}}{k!}\sum_{l=i_D+1}^{L_2^\xi}a_l^\xi(l-i_D)^k\left(\frac{\partial x}{\partial\eta}\right)_{i,j}\left(\frac{\partial^k y}{\partial\xi^k}\right)_{i_A,j}^{R-L}\\&-\frac{(\Delta\xi)^{k-1}}{k!}\sum_{m=i_D+1}^{M_2^\xi}b_m^\xi(m-i_D)^k\left(\frac{\partial y}{\partial\eta}\right)_{i,j}\left(\frac{\partial^k x}{\partial\xi^k}\right)_{i_A,j}^{R-L}\Bigg\}.\end{aligned} \tag{4.18}$$

https://doi.org/10.4208/cicp.250614.060215a Published online by Cambridge University Press

From (4.16) we know that

$$(e_{J_a})_{i,j}=(1-a)(e_{J_0})_{i,j}+a(e_{J_1})_{i,j}. \tag{4.19}$$

In particular, when $\delta_1^\xi=\delta_2^\xi$, we have

$$(e_{J_a})_{i,j}=\mathcal{O}\left((\Delta\xi)^{\min\{r,k\}},(\Delta\eta)^r\right)+\frac{(\Delta\xi)^{k-1}}{k!}g_{i,j}\sum_{l=i_D+1}^{L_2^\xi}a_l^\xi(l-i_D)^k, \tag{4.20}$$

where $g_{i,j}$ is given in (4.11). In fact, the main discretization errors of different Jacobians J_a $(0\le a\le 1)$ are all the same for the case $\delta_1^\xi=\delta_2^\xi$, but are different for the case $\delta_1^\xi\neq\delta_2^\xi$.

4.3 Spatial discretization errors

The errors of the flux part and Jacobian can be written as

$$\widetilde{A}=A+e_A,\quad \widetilde{J}=J+e_J.$$

Hence, the spatial discretization errors reads

$$e=\frac{\widetilde{A}}{\widetilde{J}}-\frac{A}{J}=\frac{A+e_A}{J+e_J}-\frac{A}{J}=\frac{Je_A-Ae_J}{J(J+e_J)}. \tag{4.21}$$

Firstly, we consider the unsteady problem $A\neq 0$. From (4.13) and (4.19), it is easy to observe that Je_A-Ae_J is of $\mathcal{O}\left((\Delta\xi)^{\min\{r,k-1\}},(\Delta\eta)^r\right)$ for NGCL-FD. Since GCL-FD satisfies CMM condition $\delta_1^\xi=\delta_2^\xi$ and $\delta_1^\eta=\delta_2^\eta$, from (4.14) and (4.20) we have

$$\begin{aligned}Je_A-Ae_J=&\frac{(\Delta\xi)^{k-1}}{k!}J_{i,j}\left[\left(\frac{\partial E}{\partial x}\right)_{i,j}+\left(\frac{\partial F}{\partial y}\right)_{i,j}\right]g_{i,j}\sum_{l=i_D+1}^{L_2^\xi}a_l^\xi(l-i_D)^k\\&-\frac{(\Delta\xi)^{k-1}}{k!}\left[\frac{\partial(Ey_\eta-Fx_\eta)}{\partial\xi}+\frac{\partial(Fx_\xi-Ey_\xi)}{\partial\eta}\right]_{i,j}g_{i,j}\sum_{l=i_D+1}^{L_2^\xi}a_l^\xi(l-i_D)^k\\&+\mathcal{O}\left((\Delta\xi)^{\min\{r,k\}},(\Delta\eta)^r\right)\\=&\mathcal{O}\left((\Delta\xi)^{\min\{r,k\}},(\Delta\eta)^r\right).\end{aligned}$$

Hence, for GCL-FD we get the error estimate

$$e_{i,j}=\mathcal{O}\left((\Delta\xi)^{\min\{r,k\}},(\Delta\eta)^r\right). \tag{4.22}$$

https://doi.org/10.4208/cicp.250614.060215a Published online by Cambridge University Press

Therefore, we have the following error estimate

$$e_{i,j}=\begin{cases}\mathcal{O}\left((\Delta\xi)^{\min\{r,k-1\}},(\Delta\eta)^r\right), & \text{for NGCL}-\text{FD},\\ \mathcal{O}\left((\Delta\xi)^{\min\{r,k\}},(\Delta\eta)^r\right), & \text{for GCL}-\text{FD}.\end{cases} \tag{4.23}$$

For steady problem, i.e., $A=0$, we have $e=e_A/(J+e_J)$ from (4.21). In this case, the spatial discretization errors are determined by the discretization errors of the flux part e_A and thus the result (4.23) also holds according to (4.15). Therefore, the result (4.23) holds for both steady and unsteady problems.

The above theoretical result can be concluded as the following theorem.

Theorem 4.1. *For C^{k-1} grid under the hypothesis of Theorem* 3.1*, the spatial discretization errors by (r)th-order finite difference schemes have the following relations:*

(i) *For nonsmooth grid ($k\leq r$), the spatial discretization accuracy approaches (k)th-order by GCL-FDr while only $(k-1)$th-order by NGCL-FDr. Thus, GCL-FDr can obtain one-order higher spatial discretization accuracy than NGCL-FDr.*

(ii) *For sufficiently smooth grid ($k>r$), the spatial discretization error term $((\widetilde{I}_x)_{i,j}E_{i,j}+(\widetilde{I}_y)_{i,j}F_{i,j})/J_{i,j}$, which is of $\mathcal{O}((\Delta\xi)^r,(\Delta\eta)^r)$, vanishes by GCL-FDr and maybe not by NGCL-FDr. Thus, GCL-FDr tends to obtain smaller spatial discretization errors than NGCL-FDr.*

For example, for a grid with $k=2$ (C^1 grid), GCL-FD2 can obtain second-order accuracy while NGCL-FD2 has only first-order accuracy.

Proposition 4.1. For C^{k-1} grid in Definition 2.3, where x,y have discontinuities in both ξ and η direction, the spatial discretization error is determined by the lowest order of discontinuities and the results in Theorem 4.1 also hold.

5 Numerical investigation

In this section, GCL errors and spatial discretization errors are tested for GCL-FD and NGCL-FD. For numerical test, we consider second-order and fourth-order finite difference operators. In Section 5.1, we make tests on grids with discontinuities in one direction to verify the results in Theorem 3.1 and Theorem 4.1. Then we choose one kind of grids with discontinuities in two directions for test in Section 5.2 to verify the results in Proposition 3.1 and Proposition 4.1.

Consider second-order and fourth-order FD operators. The general form of second-order FD operator reads

$$\delta^{\xi}E_{i,j}=\frac{\alpha}{2\Delta\xi}\left(E_{i+1,j}-E_{i-1,j}\right)+\frac{1-\alpha}{4\Delta\xi}\left(E_{i+2,j}-E_{i-2,j}\right), \tag{5.1}$$

https://doi.org/10.4208/cicp.250614.060215a Published online by Cambridge University Press

which is second-order for $\alpha \neq \frac{4}{3}$ and is fourth-order for $\alpha = \frac{4}{3}$. And the general form of fourth-order FD operator is

$$\delta^{\xi} E_{i,j} = \frac{\alpha}{2\Delta\xi}\left(E_{i+1,j} - E_{i-1,j}\right) + \frac{9-8\alpha}{20\Delta\xi}\left(E_{i+2,j} - E_{i-2,j}\right) + \frac{3\alpha-4}{30\Delta\xi}\left(E_{i+3,j} - E_{i-3,j}\right), \tag{5.2}$$

which is fourth-order for $\alpha \neq \frac{3}{2}$ and is sixth-order for $\alpha = \frac{3}{2}$. We take the operators δ_1 and δ_2 in (3.5) as the form (5.1) for second-order procedure (FD2) and the form (5.2) for fourth-order procedure (FD4). In addition, the parameter α in the operators are denoted as α_1 and α_2 for δ_1 and δ_2, respectively. For FD2 with the form (5.1), GCL-FD2 is obtained by taking the same parameter $\alpha_1 = \alpha_2 = \frac{2}{3}$ for δ_1 and δ_2, thus $\delta_1 = \delta_2$. As for NGCL-FD2, $\alpha_1 = \frac{2}{3}$ and $\alpha_2 = \frac{1}{3}$ are taken for δ_1 and δ_2, respectively, thus $\delta_1 \neq \delta_2$ and the GCL may not be hold. Similarly, for FD4 with (5.2), GCL-FD4 is obtained by taking $\alpha_1 = \alpha_2 = \frac{2}{3}$ and NGCL-FD4 by taking $\alpha_1 = \frac{2}{3}$, $\alpha_2 = \frac{1}{3}$.

5.1 Tests on grids with discontinuities in one direction

The generation of five kinds of grids with different smoothness in one direction is given in Subsection 5.1.1, and GCL errors and spatial discretization errors are given in Subsections 5.1.2 and 5.1.3, respectively. In Subsection 5.1.4, the vortex evolution problem is solved to demonstrate the errors and orders of accuracy at a fixed final time. Periodic boundary conditions are used.

5.1.1 Design of grids with different orders of smoothness

In order to test the impact of grid smoothness on GCL errors and numerical errors, grids with different orders of smoothness are generated. The grids are generated via the following coordinates transformation

$$x_{i,j} = \xi_i, \quad y_{i,j} = \eta_j + \psi_1(\xi_i)\psi_2(\eta_j), \quad \xi_i \in [-0.5, 0.5], \ \eta_j \in [-0.5, 0.5], \tag{5.3}$$

where

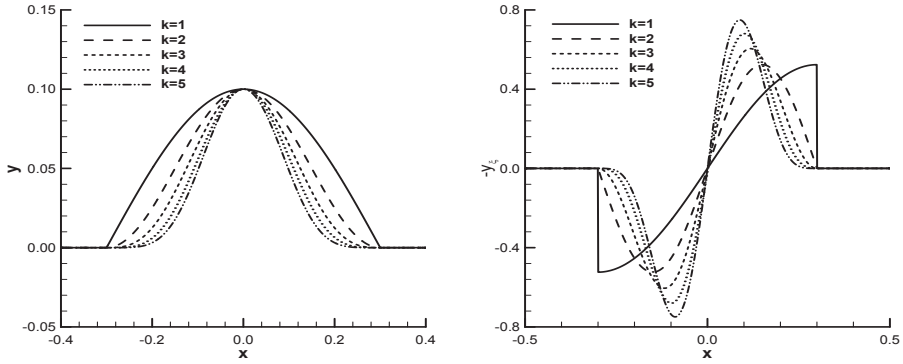
$$\psi_1(\xi_i) = \begin{cases} \sin^k\left(\frac{5\pi}{3}\xi_i + \frac{\pi}{2}\right), & |\xi_i| < 0.3, \\ 0, & |\xi_i| \geq 0.3, \end{cases} \qquad \psi_2(\eta_j) = A\sin^2\left(\pi\eta_j + \frac{\pi}{2}\right),$$

where A is amplitude of grid irregularity, $\xi_i = (i-1)\Delta\xi - 0.5$ and $\eta_j = (j-1)\Delta\eta - 0.5$. In the following, we choose $A = 0.1$. The grids with different discontinuity properties at $x = \pm 0.3$ can be produced by taking different k for $y_{i,j}$ in (5.3). These grids have the following properties:

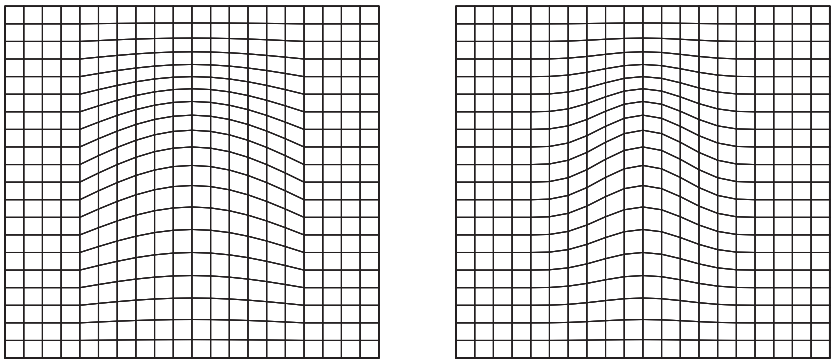
(i) Satisfying periodic boundary conditions. The grid derivatives $x_\xi, x_\eta, y_\xi, y_\eta$ and the Jacobian J are periodic in both ξ and η directions.

(ii) The parameter k determines the order of discontinuity, or more exactly, y and $\frac{\partial^p y}{\partial \eta^p}$ have kth ξ-partial discontinuities in finite points, which means that $\frac{\partial^{p+k} y}{\partial \xi^k \partial \eta^p}$ is discontinuous for $p \geq 0$ at $\xi = \pm 0.3$. In addition, x is infinite differentiable in both ξ and η directions,

https://doi.org/10.4208/cicp.250614.060215a Published online by Cambridge University Press



(a) Distribution of y along $\eta=0$ (b) Distribution of $-y_\xi$ along $\eta=0$



(c) A 20×20 Grid with $k=1$ (d) A 20×20 Grid with $k=3$

Figure 1: Distributions of y and $\widehat{\eta}_x=-y_\xi$.

which means that $\partial^{p+q}x/\partial\xi^q\partial\eta^p$ is continuous for $p\geq0$ and $q\geq0$. Moreover, since $x_\eta=0$ is satisfied everywhere, the Jacobian J is infinite differentiable in both ξ and η directions.

Figs. 1(a) and 1(b) show the distributions of $y_{i,j}$ and $\widehat{\eta}_x=-y_\xi$ along the grid line $\eta=0$ for $k=1,2,3,4,5$. We can see that the continuity property of y and y_ξ will change when the parameter k changes. For grids with the parameter k, the derivative $\frac{\partial^{k-1}y}{\partial\xi^{k-1}}$ is continuous in the whole line while $\frac{\partial^k y}{\partial\xi^k}$ is discontinuous at $x=\pm0.3$. Figs. 1(c) and 1(d) shows two 20×20 grids with $k=1$ and $k=3$, correspondingly.

The theoretical analysis has shown that GCL-FDr cannot obtain their designed accuracy order unless the grid is at least $(r-1)$th-order smooth, and NGCL-FDr requires that the grid is at least rth-order smooth. In the next two subsections, the above findings will be verified by numerical tests based on FD2 and FD4. In order to cover the grids from nonsmooth grids to sufficiently smooth grids for the two kinds of schemes, five kinds of grids with $k=1,2,3,4,5$ are generated. Table 1 shows the grid discontinuity properties and the scheme requirements of GCL-FDr and NGCL-FDr.

https://doi.org/10.4208/cicp.250614.060215a Published online by Cambridge University Press

Table 1: Relations between discontinuity orders of grids and the scheme requirements.

k	Grid smoothness at $x=\pm 0.3$		Satisfy scheme requirement or not			
	grid derivative $\partial^q y/\partial\tilde{\xi}^q$		FD2		FD4	
	continuous	discontinuous	GCL	NGCL	GCL	NGCL
1	y	$\partial y/\partial\tilde{\xi}$	No	No	No	No
2	$\partial y/\partial\tilde{\xi}$	$\partial^2 y/\partial\tilde{\xi}^2$	Yes	No	No	No
3	$\partial^2 y/\partial\tilde{\xi}^2$	$\partial^3 y/\partial\tilde{\xi}^3$	Yes	Yes	No	No
4	$\partial^3 y/\partial\tilde{\xi}^3$	$\partial^4 y/\partial\tilde{\xi}^4$	Yes	Yes	Yes	No
5	$\partial^4 y/\partial\tilde{\xi}^4$	$\partial^5 y/\partial\tilde{\xi}^5$	Yes	Yes	Yes	Yes

5.1.2 Numerical test for GCL errors

In this subsection, we test the GCL errors of NGCL-FD for five kinds of grids with different smoothness of $k=1,2,3,4,5$ given in Subsection 5.1.1. The L_1, L_2 and L_∞ GCL errors on these grids are given in Tables 2 and 3. The results are further summarized in Table 4

Table 2: GCL errors $|\widetilde{I_x}|$ for NGCL-FD2 on five kinds of grids.

NGCL	k	$N_{\tilde{\xi}}\times N_\eta$	L_1		L_2		L_∞	
			error	*order*	*error*	*order*	*error*	*order*
		300×300	1.17E-03	–	7.91E-03	–	6.85E-02	–
		500×500	7.01E-04	1.01	6.13E-03	0.50	6.85E-02	0.00
	1	800×800	4.38E-04	1.00	4.85E-03	0.50	6.85E-02	0.00
		1200×1200	2.91E-04	1.00	3.96E-03	0.50	6.85E-02	0.00
		2000×2000	1.75E-04	1.00	3.07E-03	0.50	6.85E-02	0.00
		300×300	9.24E-05	–	3.55E-04	–	4.19E-03	–
		500×500	3.33E-05	2.00	1.63E-04	1.52	2.51E-03	1.00
	2	800×800	1.30E-05	2.00	8.01E-05	1.51	1.57E-03	1.00
		1200×1200	5.79E-06	2.00	4.35E-05	1.51	1.05E-03	1.00
		2000×2000	2.08E-06	2.00	2.01E-05	1.51	6.28E-04	1.00
		300×300	1.15E-04	–	1.83E-04	–	4.97E-04	–
		500×500	4.15E-05	2.00	6.59E-05	2.00	1.80E-04	1.99
FD2	3	800×800	1.62E-05	2.00	2.58E-05	2.00	7.04E-05	2.00
		1200×1200	7.20E-06	2.00	1.15E-05	2.00	3.13E-05	2.00
		2000×2000	2.59E-06	2.00	4.13E-06	2.00	1.13E-05	2.00
		300×300	1.52E-04	–	2.49E-04	–	7.63E-04	–
		500×500	5.48E-05	2.00	8.98E-05	2.00	2.75E-04	2.00
	4	800×800	2.14E-05	2.00	3.51E-05	2.00	1.07E-04	2.00
		1200×1200	9.53E-06	2.00	1.56E-05	2.00	4.77E-05	2.00
		2000×2000	3.43E-06	2.00	5.62E-06	2.00	1.72E-05	2.00
		300×300	1.90E-04	–	3.30E-04	–	1.11E-03	–
		500×500	6.85E-05	2.00	1.19E-04	2.00	4.00E-04	2.00
	5	800×800	2.68E-05	2.00	4.65E-05	2.00	1.56E-04	2.00
		1200×1200	1.19E-05	2.00	2.07E-05	2.00	6.96E-05	2.00
		2000×2000	4.28E-06	2.00	7.44E-06	2.00	2.50E-05	2.00

https://doi.org/10.4208/cicp.250614.060215a Published online by Cambridge University Press

Table 3: GCL errors $|\widetilde{I}_x|$ for NGCL-FD4 on five kinds of grids.

NGCL	k	$N_{\tilde{\xi}} \times N_\eta$	L_1		L_2		L_∞	
			error	*order*	*error*	*order*	*error*	*order*
		300×300	9.31E-04	–	5.48E-03	–	5.48E-02	–
		500×500	5.59E-04	1.00	4.25E-03	0.50	5.48E-02	0.00
	1	800×800	3.49E-04	1.00	3.36E-03	0.50	5.48E-02	0.00
		1200×1200	2.33E-04	1.00	2.74E-03	0.50	5.48E-02	0.00
		2000×2000	1.40E-04	1.00	2.12E-03	0.50	5.48E-02	0.00
		300×300	2.44E-05	–	1.54E-04	–	1.44E-03	–
		500×500	8.78E-06	2.00	7.15E-05	1.50	8.62E-04	1.00
	2	800×800	3.43E-06	2.00	3.53E-05	1.50	5.38E-04	1.00
		1200×1200	1.52E-06	2.00	1.92E-05	1.50	3.59E-04	1.00
		2000×2000	5.48E-07	2.00	8.94E-06	1.50	2.15E-04	1.00
		300×300	9.60E-07	–	5.46E-06	–	4.86E-05	–
		500×500	1.95E-07	3.12	1.52E-06	2.51	1.74E-05	2.02
FD4	3	800×800	4.59E-08	3.08	4.68E-07	2.50	6.76E-06	2.01
		1200×1200	1.33E-08	3.05	1.70E-07	2.50	3.00E-06	2.00
		2000×2000	2.83E-09	3.03	4.73E-08	2.50	1.08E-06	2.00
		300×300	3.72E-07	–	6.85E-07	–	5.56E-06	–
		500×500	4.84E-08	3.99	1.02E-07	3.73	1.20E-06	3.00
	4	800×800	7.40E-09	4.00	1.81E-08	3.67	2.94E-07	3.00
		1200×1200	1.46E-09	4.00	4.16E-09	3.63	8.71E-08	3.00
		2000×2000	1.90E-10	4.00	6.64E-10	3.59	1.88E-08	3.00
		300×300	4.98E-07	–	8.17E-07	–	2.60E-06	–
		500×500	6.47E-08	4.00	1.06E-07	4.00	3.37E-07	4.00
	5	800×800	9.87E-09	4.00	1.62E-08	4.00	5.15E-08	4.00
		1200×1200	1.95E-09	4.00	3.20E-09	4.00	1.02E-08	4.00
		2000×2000	2.53E-10	4.00	4.15E-10	4.00	1.32E-09	4.00

to show the relation between the convergence rate of GCL errors, the grid discontinuity order k, and the accuracy order r of difference operators.

Firstly, we have a close look at the relation between grid smoothness and the convergent order of GCL errors. For the grids with $k=1$, we can see from Tables 2 and 3 that the order of L_1, L_2 and L_∞ GCL errors are 1, 0.5 and 0, respectively, for both NGCL-FD2 and NGCL-FD4. Similarly, for the other four kinds of grids, the L_1, L_2 and L_∞ GCL errors of NGCL-FDr ($r=2$ or $r=4$) converge in the rates of $\min(k,r)$, $\min(k-0.5,r)$ and $\min(k-1,r)$, respectively. The L_∞ errors agree with the theoretical results (3.9).

Secondly, It is worth noting that the GCL errors of the fourth-order scheme are generally lower than that of the second-order scheme, although the GCL errors of the two schemes show similar convergence rate on non-sufficiently smooth grids. Taking the grids with k=2 for an example, although the convergence rates of NGCL-FD2 and NGCL-FD4 are the same, the latter one produces smaller GCL errors than the former.

Thirdly, grids with $k=r+1$ (C^r grid) are sufficiently smooth for NGCL-FDr from the

https://doi.org/10.4208/cicp.250614.060215a Published online by Cambridge University Press

Table 4: The correlation among the convergent rate of GCL errors $|\widetilde{I_x}|$, the grid continuity order k, and the accuracy order r of difference operators.

grid property			$\|\widetilde{I_x}\|$					
k	grid coordinate	grid derivative	NGCL-FD2 ($r=2$)			NGCL-FD4 ($r=4$)		
	order of continuity	order of continuity	L_1	L_2	L_∞	L_1	L_2	L_∞
1	1st-order	zero-order	1.0	0.5	0.0	1.0	0.5	0.0
2	2nd-order	1st-order	2.0	1.5	1.0	2.0	1.5	1.0
3	3th-order	2nd-order	**2.0**	**2.0**	**2.0**	3.0	2.5	2.0
4	4th-order	3th-order	2.0	2.0	2.0	4.0	3.5	3.0
5	5th-order	4th-order	2.0	2.0	2.0	**4.0**	**4.0**	**4.0**

aspect of GCL errors. For example, the grids with k=3 are smooth enough for NGCL-FD2 to obtain second-order accuracy from the aspect of all the $L_m(m=1,2,\cdots,\infty)$ GCL errors, and the grids with $k=5$ are smooth enough for the NGCL-FD4.

5.1.3 Numerical test for spatial discretization errors

In this subsection, spatial discretization errors of GCL-FD and NGCL-FD are tested on the five kinds of grids given in Subsection 5.1.1. Since y is discontinuous in η direction, we check the spatial discretization errors of $\frac{\partial E}{\partial x}=\frac{A_E}{J}$ and choose $E(x,y)=\sin(2\pi x)\sin(2\pi y)$.

The discretization errors and the accuracy orders for FD4 is listed in Tables 5 and 6. Firstly, when the grids are first-order discontinuous ($k=1$), the orders of L_1,L_2 and L_∞ errors are 2, 1.5 and 1 for GCL-FD4, but 1, 0.5 and 0 for NGCL-FD4. The L_∞ errors of NGCL-FD4 can not converge to zero as refining the grids because the discrete version of the spatial terms in Eq. (4.2) is inconsistent with Eq. (4.1) due to the strong non-smoothness of the grids. Secondly, it can be concluded that the orders of L_1, L_2 and L_∞ errors are $\min(k+1,r)$, $\min(k+0.5,r)$ and $\min(k,r)$ for GCL-FDr, but $\min(k,r)$, $\min(k-0.5,r)$ and $\min(k-1,r)$ for NGCL-FDr. In order to facilitate the analysis, numerical spatial errors by NGCL-FD4 and GCL-FD4 are also plotted together as shown in Fig. 2. This result indicates that for nonsmooth grids ($k\leq r$), the GCL-FDr has one order higher spatial accuracy than NGCL-FDr. Thirdly, to obtain the designed accuracy orders, the grids with $k=r$ (C^{r-1} grid) are smooth enough for GCL-FDr schemes while the grids with $k=r+1$ (C^r grid) are smooth enough for NGCL-FDr schemes. Fourthly, we can see from the results of the case $k=5$ that satisfying the GCL can still reduce the discretization errors for sufficiently smooth grids, which agrees with Theorem 4.1.

FD2 is also tested and the results are not listed here. It can be found that FD2 also have the above four properties. Table 7 gives the relation between numerical errors, the grid smoothness, and the accuracy orders of difference operator for FD2 and FD4. In addition, although GCL-FD2 and GCL-FD4 have the same accuracy on the grids with $k=1$, the former has larger numerical errors than the latter. This is similar to the comparison between NGCL-FD2 and NGCL-FD4. The results indicate that high-order schemes might

https://doi.org/10.4208/cicp.250614.060215a Published online by Cambridge University Press

Table 5: Numerical errors $\left|\frac{\partial E}{\partial x}^{N}-\frac{\partial E}{\partial x}^{exact}\right|$ for GCL-FD4 on five kinds of grids.

FD4	k	$N_\xi \times N_\eta$	L_1 error	L_1 order	L_2 error	L_2 order	L_∞ error	L_∞ order
GCL	1	300×300	5.81E-05	–	4.26E-04	–	8.40E-03	–
		500×500	2.08E-05	2.01	1.98E-04	1.50	5.08E-03	0.99
		800×800	8.08E-06	2.01	9.76E-05	1.50	3.19E-03	0.99
		1200×1200	3.59E-06	2.00	5.31E-05	1.50	2.13E-03	0.99
		2000×2000	1.29E-06	2.00	2.47E-05	1.50	1.28E-03	1.00
	2	300×300	2.11E-06	–	1.00E-05	–	1.48E-04	–
		500×500	3.86E-07	3.33	2.75E-06	2.53	5.02E-05	2.12
		800×800	8.45E-08	3.23	8.46E-07	2.51	1.89E-05	2.07
		1200×1200	2.34E-08	3.16	3.07E-07	2.50	8.34E-06	2.02
		2000×2000	4.78E-09	3.11	8.55E-08	2.50	3.00E-06	2.00
	3	300×300	1.45E-06	–	2.46E-06	–	1.09E-05	–
		500×500	1.91E-07	3.98	3.27E-07	3.95	2.45E-06	2.92
		800×800	2.93E-08	3.98	5.17E-08	3.93	6.10E-07	2.96
		1200×1200	5.81E-09	3.99	1.07E-08	3.90	1.83E-07	2.97
		2000×2000	7.56E-10	3.99	1.49E-09	3.85	3.99E-08	2.98
	4	300×300	1.92E-06	–	3.65E-06	–	1.86E-05	–
		500×500	2.49E-07	4.00	4.75E-07	4.00	2.42E-06	3.99
		800×800	3.81E-08	4.00	7.25E-08	4.00	3.69E-07	4.00
		1200×1200	7.52E-09	4.00	1.43E-08	4.00	7.30E-08	4.00
		2000×2000	9.75E-10	4.00	1.86E-09	4.00	9.46E-09	4.00
	5	300×300	2.53E-06	–	5.20E-06	–	2.88E-05	–
		500×500	3.28E-07	3.99	6.77E-07	3.99	3.74E-06	3.99
		800×800	5.02E-08	4.00	1.03E-07	4.00	5.72E-07	4.00
		1200×1200	9.91E-09	4.00	2.04E-08	4.00	1.13E-07	4.00
		2000×2000	1.28E-09	4.00	2.65E-09	4.00	1.47E-08	4.00

be superior to low-order schemes in reducing numerical errors even for grids with first-order discontinuity.

5.1.4 Vortex evolution problem

In this subsection, GCL-FD and NGCL-FD are applied to solve isentropic moving vortex problem on five kinds of grids given in Subsection 5.1.1 with initial conditions

$$\rho=\left(1-\frac{\gamma-1}{4\alpha\gamma}\Phi^2\right)^{(\gamma-1)},\quad u=a+\frac{y-y_c}{r_c}\Phi,\quad v=b-\frac{x-x_c}{r_c}\Phi,\quad p=\rho^\gamma,$$

where $\gamma=1.4$ is the specific heat ratio $\alpha=1.2$ is the parameter of the length scale of vortex decay. Here we define a function $\Phi=\varepsilon e^{\alpha\left(1-d^2\right)}$ with the vortex strength $\varepsilon=0.2$, $d=\frac{r}{r_c}$, $r=\sqrt{(x-x_c)^2+(y-y_c)^2}$, the vortex core width $r_c=0.1$ and the initial center of the vortex $(x_c,y_c)=(0,0)$. $(a,b)=(1,0)$ is the moving speed of the isentropic vortex.

https://doi.org/10.4208/cicp.250614.060215a Published online by Cambridge University Press

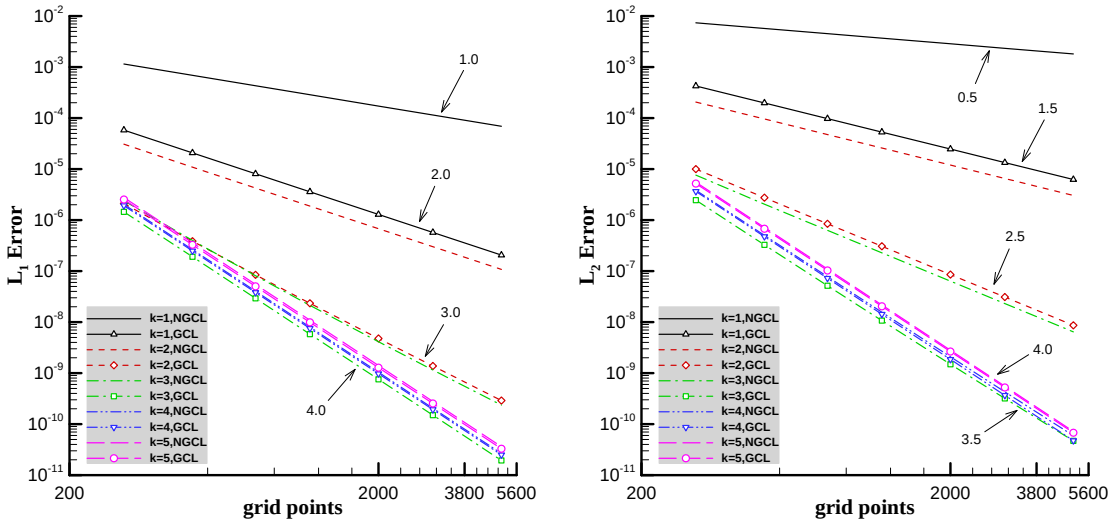
Table 6: Numerical errors $\left|\frac{\partial E}{\partial x}^{N}-\frac{\partial E}{\partial x}^{exact}\right|$ for NGCL-FD4 on five kinds of grids.

FD4	k	$N_{\tilde{\xi}}\times N_{\eta}$	L_1 *error*	L_1 *order*	L_2 *error*	L_2 *order*	L_∞ *error*	L_∞ *order*
NGCL	1	300×300	1.15E-03	–	7.37E-03	–	1.09E-01	–
		500×500	6.89E-04	1.00	5.71E-03	0.50	1.07E-01	0.04
		800×800	4.31E-04	1.00	4.52E-03	0.50	1.06E-01	0.02
		1200×1200	2.87E-04	1.00	3.69E-03	0.50	1.06E-01	0.01
		2000×2000	1.72E-04	1.00	2.86E-03	0.50	1.05E-01	0.01
	2	300×300	3.08E-05	–	2.06E-04	–	2.83E-03	–
		500×500	1.09E-05	2.03	9.61E-05	1.50	1.68E-03	1.03
		800×800	4.25E-06	2.01	4.75E-05	1.50	1.04E-03	1.02
		1200×1200	1.88E-06	2.00	2.59E-05	1.50	6.90E-04	1.01
		2000×2000	6.78E-07	2.00	1.20E-05	1.50	4.12E-04	1.01
	3	300×300	2.39E-06	–	7.62E-06	–	9.72E-05	–
		500×500	4.00E-07	3.50	2.05E-06	2.57	3.38E-05	2.07
		800×800	8.11E-08	3.39	6.30E-07	2.51	1.30E-05	2.03
		1200×1200	2.13E-08	3.30	2.28E-07	2.50	5.77E-06	2.01
		2000×2000	4.12E-09	3.21	6.36E-08	2.50	2.07E-06	2.01
	4	300×300	2.03E-06	–	3.84E-06	–	1.85E-05	–
		500×500	2.64E-07	3.99	5.03E-07	3.98	2.40E-06	4.00
		800×800	4.05E-08	3.99	7.79E-08	3.97	5.45E-07	3.15
		1200×1200	8.01E-09	4.00	1.56E-08	3.96	1.63E-07	2.98
		2000×2000	1.04E-09	4.00	2.09E-09	3.94	3.54E-08	2.99
	5	300×300	2.77E-06	–	5.53E-06	–	2.85E-05	–
		500×500	3.60E-07	3.99	7.18E-07	3.99	3.71E-06	3.99
		800×800	5.50E-08	4.00	1.10E-07	4.00	5.67E-07	4.00
		1200×1200	1.09E-08	4.00	2.17E-08	4.00	1.12E-07	4.00
		2000×2000	1.41E-09	4.00	2.81E-09	4.00	1.45E-08	4.00

Table 7: Accuracy of numerical errors.

k	$\left\|\frac{\partial E}{\partial x}^{N}-\frac{\partial E}{\partial x}^{exact}\right\|$											
	FD2						FD4					
	GCL			NGCL			GCL			NGCL		
	L_1	L_2	L_∞	L_1	L_2	L_∞	L_1	L_2	L_∞	L_1	L_2	L_∞
1	2.0	1.5	1.0	1.0	0.5	0.0	2.0	1.5	1.0	1.0	0.5	0.0
2	**2.0**	**2.0**	**2.0**	2.0	1.5	1.0	3.0	2.5	2.0	2.0	1.5	1.0
3	2.0	2.0	2.0	**2.0**	**2.0**	**2.0**	4.0	3.5	3.0	3.0	2.5	2.0
4	2.0	2.0	2.0	2.0	2.0	2.0	**4.0**	**4.0**	**4.0**	4.0	3.5	3.0
5	2.0	2.0	2.0	2.0	2.0	2.0	4.0	4.0	4.0	**4.0**	**4.0**	**4.0**

https://doi.org/10.4208/cicp.250614.060215a Published online by Cambridge University Press



(a) L_1 Error

(b) L_2 Error

(c) L_∞ Error

Figure 2: Numerical errors $\left|\frac{\partial E}{\partial x}^N - \frac{\partial E}{\partial x}^{exact}\right|$ with FD4 on four kinds of grids.

Firstly, the problem is solved in the area $[-0.5,0.5]\times[-0.5,0.5]$ till $T=1.0$. Tables 8 and 9 gives numerical accuracy of density for GCL-FD4 and NGCL-FD4, respectively. It can be seen that GCL-FD4 performs at nearly second order accuracy on grids with $k=1$ while NGCL-FD4 at nearly first order accuracy. Thus GCL-FD4 has one order higher accuracy than NGCL-FD4. In addition GCL-FD4 has second order higher order accuracy

https://doi.org/10.4208/cicp.250614.060215a Published online by Cambridge University Press

Table 8: Numerical errors $|u^N - u^{exact}|$ of GCL-FD4 at time $T=1$.

FD4	k	$N_\xi \times N_\eta$	L_1 *error*	L_1 *order*	L_2 *error*	L_2 *order*	L_∞ *error*	L_∞ *order*
GCL	1	300×300	4.91E-06	–	9.51E-06	–	1.67E-04	–
		500×500	1.46E-06	2.38	3.15E-06	2.16	6.14E-05	1.96
		800×800	4.77E-07	2.37	1.11E-06	2.22	2.63E-05	1.81
		1200×1200	1.80E-07	2.40	4.42E-07	2.27	9.81E-06	2.43
		2000×2000	4.71E-08	2.63	1.28E-07	2.42	2.84E-06	2.43
	2	300×300	5.01E-07	–	1.76E-06	–	2.41E-05	–
		500×500	6.96E-08	3.86	2.32E-07	3.97	3.25E-06	3.92
		800×800	1.16E-08	3.82	3.60E-08	3.96	4.96E-07	4.00
		1200×1200	2.53E-09	3.74	7.37E-09	3.92	9.82E-08	4.00
		2000×2000	3.70E-10	3.77	1.03E-09	3.85	1.48E-08	3.70
	3	300×300	4.61E-07	–	1.75E-06	–	2.42E-05	–
		500×500	5.94E-08	4.01	2.29E-07	3.99	3.03E-06	4.07
		800×800	9.08E-09	3.99	3.50E-08	3.99	4.74E-07	3.94
		1200×1200	1.80E-09	4.00	6.92E-09	4.00	9.35E-08	4.01
		2000×2000	2.33E-10	4.00	8.97E-10	4.00	1.21E-08	4.00
	4	300×300	4.87E-07	–	1.77E-06	–	2.43E-05	–
		500×500	6.26E-08	4.02	2.31E-07	3.99	3.45E-06	3.82
		800×800	9.56E-09	4.00	3.53E-08	3.99	5.29E-07	3.99
		1200×1200	1.89E-09	4.00	6.97E-09	4.00	1.05E-07	4.00
		2000×2000	2.45E-10	4.00	9.04E-10	4.00	1.36E-08	4.00
	5	300×300	5.22E-07	–	1.79E-06	–	2.66E-05	–
		500×500	6.72E-08	4.02	2.34E-07	3.99	3.80E-06	3.81
		800×800	1.03E-08	4.00	3.57E-08	3.99	5.86E-07	3.98
		1200×1200	2.03E-09	4.00	7.06E-09	4.00	1.16E-07	4.00
		2000×2000	2.63E-10	4.00	9.16E-10	4.00	1.50E-08	4.00

than NGCL-FD4 on grids with $k=2$. Moreover, GCL-FD4 has a bit smaller error than NGCL-FD4 for $k=3$ and has nearly the same errors for $k=4,5$.

Secondly, we solve the problem till $T=2.0$ to see the time variation of orders for GCL-FD4 and NGCL-FD4 on grids with $k=1$. And numerical errors on two grids with 500×500 and 800×800 grid points are used to calculate numerical orders. From Fig. 3 we can see that GCL-FD4 has one order higher accuracy than NGCL-FD4 with respect to L_1 order and L_2 order. As for L_∞ order, both schemes has large vibration. The former one always has higher order accuracy than the latter one and the exceeding order vibrates with time. Moreover, we can see from Fig. 4 that both the errors and the area influenced by nonsmooth grid for GCL-FD4 are much smaller than that for NGCL-FD4.

Therefore, GCL-FD has superiority over NGCL-FD4 in spatial accuracy at a fixed final time. In addition, the exceeding order of GCL-FD4 over NGCL-FD4 may be different for different grids. The reason may be that the influence of local truncation errors near discontinuous points on global errors may rely on two aspects which are properties of the

https://doi.org/10.4208/cicp.250614.060215a Published online by Cambridge University Press

Table 9: Numerical errors $|u^N - u^{exact}|$ of NGCL-FD4 at time $T=1$.

FD4	k	$N_\xi \times N_\eta$	L_1 *error*	L_1 *order*	L_2 *error*	L_2 *order*	L_∞ *error*	L_∞ *order*
NGCL	1	300×300	1.16E-04	–	1.59E-04	–	7.62E-04	–
		500×500	5.44E-05	1.49	7.41E-05	1.49	4.01E-04	1.26
		800×800	2.97E-05	1.29	4.39E-05	1.12	2.15E-04	1.33
		1200×1200	1.70E-05	1.38	2.58E-05	1.31	1.43E-04	1.00
		2000×2000	9.15E-06	1.21	1.47E-05	1.10	7.74E-05	1.20
	2	300×300	3.36E-06	–	4.42E-06	–	2.57E-05	–
		500×500	9.13E-07	2.55	1.29E-06	2.41	5.95E-06	2.87
		800×800	3.22E-07	2.22	4.66E-07	2.17	2.17E-06	2.14
		1200×1200	1.29E-07	2.26	2.00E-07	2.09	9.53E-07	2.03
		2000×2000	3.87E-08	2.35	6.22E-08	2.29	3.40E-07	2.01
	3	300×300	4.76E-07	–	1.76E-06	–	2.42E-05	–
		500×500	6.25E-08	3.97	2.29E-07	3.99	3.03E-06	4.07
		800×800	9.90E-09	3.92	3.51E-08	3.99	4.76E-07	3.94
		1200×1200	2.05E-09	3.89	6.96E-09	3.99	9.38E-08	4.00
		2000×2000	2.91E-10	3.82	9.10E-10	3.98	1.22E-08	4.00
	4	300×300	4.87E-07	–	1.77E-06	–	2.43E-05	–
		500×500	6.26E-08	4.02	2.31E-07	3.99	3.45E-06	3.82
		800×800	9.56E-09	4.00	3.53E-08	3.99	5.29E-07	3.99
		1200×1200	1.89E-09	4.00	6.97E-09	4.00	1.04E-07	4.00
		2000×2000	2.45E-10	4.00	9.04E-10	4.00	1.36E-08	4.00
	5	300×300	5.23E-07	–	1.79E-06	–	2.66E-05	–
		500×500	6.72E-08	4.02	2.34E-07	3.99	3.80E-06	3.81
		800×800	1.03E-08	4.00	3.57E-08	3.99	5.85E-07	3.98
		1200×1200	2.03E-09	4.00	7.06E-09	4.00	1.16E-07	3.99
		2000×2000	2.63E-10	4.00	9.16E-10	4.00	1.50E-08	4.00

grid (discontinuity order and discontinuity distribution) and properties of the solution (solution distribution and solution evolution).

5.2 Tests on grids with discontinuities in two directions

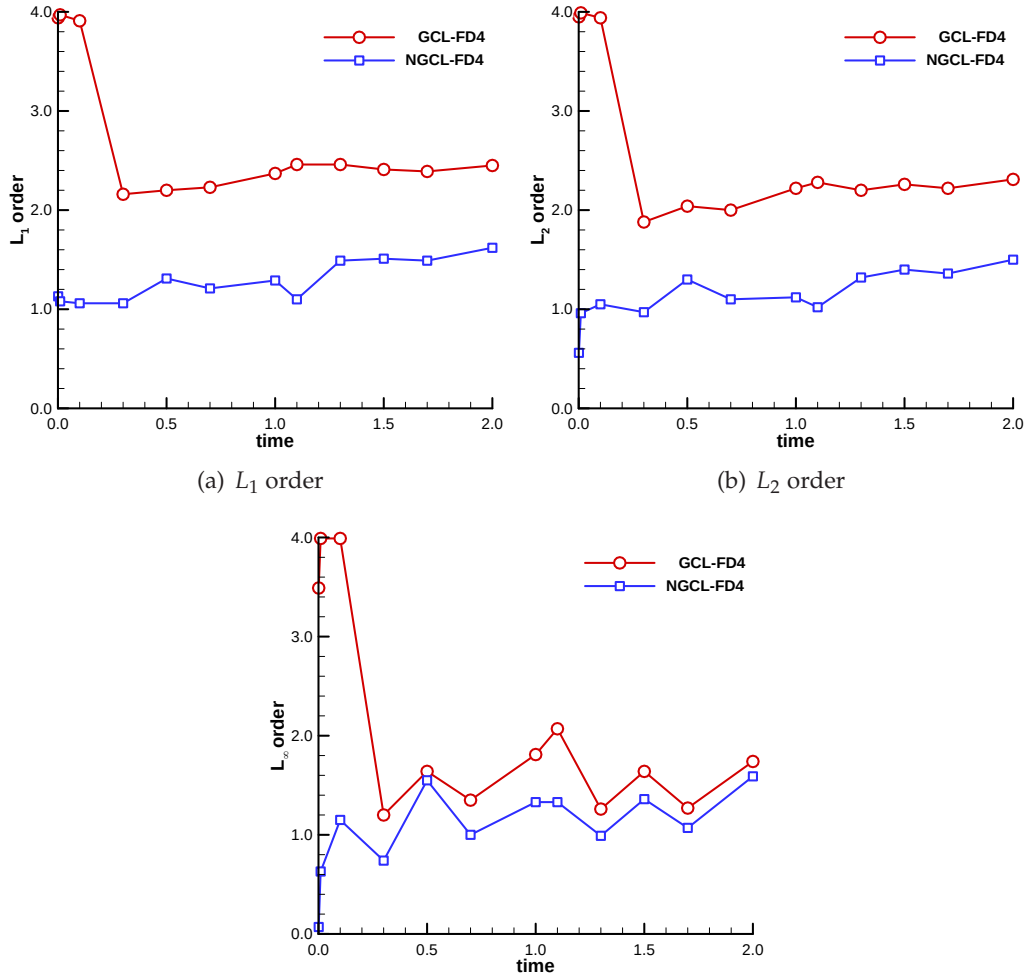
In this subsection, we test GCL errors and numerical errors on grids with discontinuities in two directions. The grids are generated via the following coordinates transformation

$$x_{i,j}=\xi_i,\quad y_{i,j}=\eta_j+\psi_1(\xi_i)\psi_2(\eta_j),\quad \xi_i\in[-0.5,0.5],\ \eta_j\in[-0.5,0.5]. \tag{5.4}$$

where

$$\psi_1(\xi_i)=\begin{cases}\sin^{k_\xi}\left(\frac{5\pi}{3}\xi_i+\frac{\pi}{2}\right), & |\xi_i|<0.3,\\ 0, & |\xi_i|\geq 0.3,\end{cases}\qquad \psi_2(\eta_j)=\begin{cases}\sin^{k_\eta}\left(\frac{5\pi}{3}\eta_j+\frac{\pi}{2}\right), & |\eta_j|<0.3,\\ 0, & |\eta_j|\geq 0.3.\end{cases}$$

https://doi.org/10.4208/cicp.250614.060215a Published online by Cambridge University Press



(a) L_1 order (b) L_2 order

(c) L_∞ order

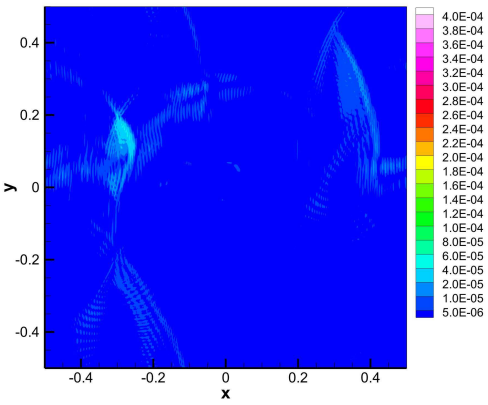
Figure 3: Time variation of numerical order for GCL-FD and NGCL-FD.

Here k_ξ and k_η denote the order of discontinuity of y in ξ and η direction, respectively. We test the case $k_\xi=2$ and $k_\eta=4$.

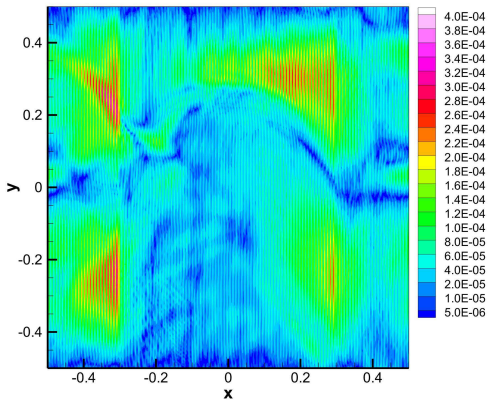
The GCL errors of NGCL-FD are summarized in Table 10. We can see that the order of L_1, L_2 and L_∞ GCL errors are 2, 1.5 and 1, respectively, for both NGCL-FD2 and NGCL-FD4. This result indicates that the GCL errors of NGCL-FD are determined by the lower order of discontinuity order $k=\min(k_\xi,k_\eta)$ and is consistent with Proposition 3.1.

Tables 11 and 12 give the spatial discretization errors of GCL-FD and NGCL-FD. It can be concluded that the orders of L_1, L_2 and L_∞ errors are $\min(k+1,r)$, $\min(k+0.5,r)$ and $\min(k,r)$ for GCL-FDr, but $\min(k,r)$, $\min(k-0.5,r)$ and $\min(k-1,r)$ for NGCL-FDr. This result agrees with Proposition 4.1.

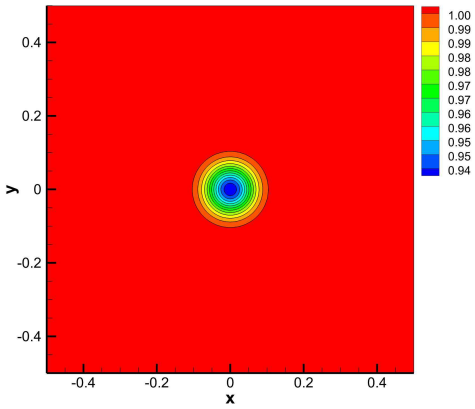
https://doi.org/10.4208/cicp.250614.060215a Published online by Cambridge University Press



(a) Error distribution of density for GCL-FD4



(b) Error distribution of density for NGCL-FD4



(c) Density distribution for NGCL-FD4

Figure 4: Error distribution of density for GCL-FD4 and NGCL-FD4 at time $T=2$ in solving vortex problem on 500×500 grid with $k=1$.

6 Concluding remarks

In the present work, the impact of grid discontinuities on the GCL errors and spatial discretization errors is analyzed theoretically and numerically to explore how GCL works in finite difference method. The GCL errors are proved to be zero for GCL-FD. However, for NGCL-FD, the GCL errors are related to grid smoothness. For C^{k-1} grids and rth-order finite difference operators, the GCL errors of NGCL-FD are approaching to zero with refining grids at $\min\{r,k-1\}$th-order convergence rate. The convergence rate of spatial discretization errors is $\min\{r,k\}$th order for GCL-FD but $\min\{r,k-1\}$th order for

https://doi.org/10.4208/cicp.250614.060215a Published online by Cambridge University Press

Table 10: GCL errors $\left|\widetilde{I_x}\right|$ for NGCL-FD2 and NGCL-FD4 on grids with $k_{\tilde{\xi}}=2$ and $k_\eta=4$.

NGCL	$N_{\tilde{\xi}}\times N_\eta$	L_1		L_2		L_∞	
		error	*order*	*error*	*order*	*error*	*order*
FD2	300×300	1.08E-04	–	4.11E-04	–	6.91E-03	–
	500×500	3.90E-05	2.00	1.85E-04	1.57	4.14E-03	1.00
	800×800	1.52E-05	2.00	8.95E-05	1.54	2.59E-03	1.00
	1200×1200	6.77E-06	2.00	4.81E-05	1.53	1.73E-03	1.00
	2000×2000	2.44E-06	2.00	2.22E-05	1.52	1.04E-03	1.00
FD4	300×300	1.64E-05	–	1.60E-04	–	2.07E-03	–
	500×500	5.87E-06	2.01	7.41E-05	1.50	1.24E-03	1.00
	800×800	2.29E-06	2.01	3.66E-05	1.50	7.77E-04	1.00
	1200×1200	1.02E-06	2.00	1.99E-05	1.50	5.18E-04	1.00
	2000×2000	3.66E-07	2.00	9.27E-06	1.50	3.11E-04	1.00

Table 11: Numerical errors $\left|\frac{\partial E}{\partial x}^N-\frac{\partial E}{\partial x}^{exact}\right|$ for GCL-FD2 and NGCL-FD2 on grids with $k_{\tilde{\xi}}=2$ and $k_\eta=4$.

FD2	$N_{\tilde{\xi}}\times N_\eta$	L_1		L_2		L_∞	
		error	*order*	*error*	*order*	*error*	*order*
GCL	300×300	2.67E-04	–	3.67E-04	–	1.22E-03	–
	500×500	9.60E-05	2.00	1.32E-04	2.00	4.40E-04	2.00
	800×800	3.75E-05	2.00	5.17E-05	2.00	1.72E-04	2.00
	1200×1200	1.67E-05	2.00	2.30E-05	2.00	7.65E-05	2.00
	2000×2000	6.01E-06	2.00	8.28E-06	2.00	2.75E-05	2.00
NGCL	300×300	3.34E-04	–	5.31E-04	–	8.92E-03	–
	500×500	1.21E-04	1.99	2.06E-04	1.85	5.40E-03	0.98
	800×800	4.72E-05	2.00	8.84E-05	1.80	3.39E-03	0.99
	1200×1200	2.10E-05	2.00	4.36E-05	1.75	2.26E-03	0.99
	2000×2000	7.56E-06	2.00	1.84E-05	1.69	1.36E-03	1.00

NGCL-FD. Then for non-sufficiently smooth grids with $k<r+1$, GCL-FD has one order higher spatial accuracy than NGCL-FD. If the grid is sufficiently smooth, namely $k\geq r+1$, both GCL-FD and NGCL-FD can obtain rth-order spatial accuracy, but the former is proved to produce smaller numerical errors than the latter. It can be concluded that satisfying the GCL helps FDSs to obtain one more order of accuracy for non-sufficiently smooth grids and reduce discretization errors for sufficiently smooth grid.

The following two issues are worth to be emphasized: (i) Satisfying the GCL can reduce the grid requirement of FDSs. GCL-FDr only needs a C^{r-1} grid while NGCL-FDr needs a C^r grid to obtain their rth-order accuracy. Thus, from the viewpoint of grid generation, satisfying the GCL can reduce the difficulties on grid generation for high-order FDSs when complex configurations are involved. (ii) Satisfying the GCL can make finite difference equation be consistent with the corresponding differential equation. For C^0 grids, GCL-FD still has first-order accuracy and thus satisfies consistent condition.

https://doi.org/10.4208/cicp.250614.060215a Published online by Cambridge University Press

Table 12: Numerical errors $\left|\frac{\partial E}{\partial x}^{N}-\frac{\partial E}{\partial x}^{exact}\right|$ for GCL-FD4 and NGCL-FD4 on grids with $k_\xi=2$ and $k_\eta=4$.

FD4	$N_\xi\times N_\eta$	L_1		L_2		L_∞	
		error	*order*	*error*	*order*	*error*	*order*
GCL	300×300	5.61E-07	–	2.96E-06	–	7.31E-05	–
	500×500	9.14E-08	3.55	7.97E-07	2.57	2.56E-05	2.06
	800×800	1.82E-08	3.43	2.44E-07	2.52	9.91E-06	2.02
	1200×1200	4.71E-09	3.33	8.85E-08	2.51	4.39E-06	2.01
	2000×2000	9.00E-10	3.24	2.47E-08	2.50	1.57E-06	2.01
NGCL	300×300	1.21E-05	–	1.31E-04	–	4.54E-03	–
	500×500	4.27E-06	2.03	6.10E-05	1.50	2.73E-03	1.00
	800×800	1.66E-06	2.01	3.02E-05	1.50	1.71E-03	1.00
	1200×1200	7.35E-07	2.00	1.64E-05	1.50	1.14E-03	1.00
	2000×2000	2.64E-07	2.00	7.63E-06	1.50	6.83E-04	1.00

However, NGCL-FD only have zeroth-order accuracy, and the L_∞ error dose not decrease to zero because the local truncation errors of the difference equation cannot converge to zero as the grid is refined. This means that the finite difference equation of the NGCL-FD is no longer consistent with the corresponding differential equation on C^0 grids.

FDSs satisfying the GCL can obtain better solutions because the spatial discretization errors are reduced. Some researches show the numerical stability of finite difference method can also be improved by following GCL. Therefore, More attention will be paid to the influence of the GCL on the numerical stability in our future works.

Acknowledgments

This study was supported by the project of National Basic Research Program of China (Grant No. 2009CB723800), National Natural Science Foundation of China (Grant Nos. 11372342, 11072259 and 11301525) and the foundation of State Key Laboratory of Aerodynamics (Grant No. JBKY11030902). We would like to thank Dr. Guohua Tu for his valuable suggestions on improving this manuscript.

Appendix: Discretization errors of the E flux part

By using the operators in (3.5), the discretization form of the E-flux part (4.6) reads

$$\left(\widetilde{A_E}\right)_{i,j}=\frac{1}{\Delta\xi}\sum_{l=-L_1^\xi}^{L_2^\xi}a_l^\xi\left(E_{i+l,j}\delta_2^\eta y_{i+l,j}-E_{i,j}\delta_2^\eta y_{i+l,j}+E_{i,j}\delta_2^\eta y_{i+l,j}-E_{i,j}\delta_2^\eta y_{i,j}\right)$$
$$-\frac{1}{\Delta\eta}\sum_{l=-L_1^\eta}^{L_2^\eta}a_l^\eta\left(E_{i,j+l}\delta_2^\xi y_{i,j+l}-E_{i,j}\delta_2^\xi y_{i,j+l}+E_{i,j}\delta_2^\xi y_{i,j+l}-E_{i,j}\delta_2^\xi y_{i,j}\right)$$

https://doi.org/10.4208/cicp.250614.060215a Published online by Cambridge University Press

$$=\frac{1}{\Delta\xi}\sum_{l=-L_1^\xi}^{L_2^\xi}a_l^\xi\left(E_{i+l,j}-E_{i,j}\right)\delta_2^\eta y_{i+l,j}-\frac{1}{\Delta\eta}\sum_{l=-L_1^\eta}^{L_2^\eta}a_l^\eta\left(E_{i,j+l}-E_{i,j}\right)\delta_2^\xi y_{i,j+l}+E_{i,j}(\widetilde{I}_x)_{i,j}, \tag{A.1}$$

where we have used (3.4) to get the last equality. Using (2.10), we have

$$\begin{aligned}\left(\widetilde{A_E}\right)_{i,j}=&(\widetilde{I}_x)_{i,j}E_{i,j}+\frac{1}{\Delta\xi}\sum_{l=-L_1^\xi}^{L_2^\xi}a_l^\xi(E_{i+l,j}-E_{i,j})\sum_{m=-M_1^\eta}^{M_2^\eta}b_m^\eta\sum_{p=1}^{\infty}\frac{m^p(\Delta\eta)^{p-1}}{p!}\left(\frac{\partial^p y}{\partial\eta^p}\right)_{i+l,j}\\&-\sum_{l=-L_1^\eta}^{L_2^\eta}a_l^\eta\sum_{p=1}^{\infty}\frac{l^p(\Delta\eta)^{p-1}}{p!}\left(\frac{\partial^p E}{\partial\eta^p}\right)_{i,j}\left\{\sum_{m=-M_1^\xi}^{M_2^\xi}b_m^\xi\sum_{q=1}^{\infty}\frac{m^q(\Delta\xi)^{q-1}}{q!}\left(\frac{\partial^q y}{\partial\xi^q}\right)_{i,j+l}\right.\\&\left.+\sum_{m=i_D+1}^{M_2^\xi}b_m^\xi\sum_{q=1}^{\infty}\frac{(m-i_D)^q(\Delta\xi)^{q-1}}{q!}\left(\frac{\partial^q y}{\partial\xi^q}\right)_{i_A,j+l}^{R-L}\right\}.\end{aligned} \tag{A.2}$$

Getting the main error terms according to the coefficient relations, we have

$$\begin{aligned}\left(\widetilde{A_E}\right)_{i,j}=&\frac{1}{\Delta\xi}\sum_{l=-L_1^\xi}^{L_2^\xi}a_l^\xi(E_{i+l,j}-E_{i,j})\left(\frac{\partial y}{\partial\eta}\right)_{i+l,j}-\left(\frac{\partial E}{\partial\eta}\right)_{i,j}\left(\frac{\partial y}{\partial\xi}\right)_{i,j}+(\widetilde{I}_x)_{i,j}E_{i,j}\\&-\left(\frac{\partial E}{\partial\eta}\right)_{i,j}\sum_{m=i_D+1}^{M_2^\xi}b_m^\xi\sum_{q=1}^{\infty}\frac{(m-i_D)^q(\Delta\xi)^{q-1}}{q!}\left(\frac{\partial^q y}{\partial\xi^q}\right)_{i_A,j}^{R-L}+\mathcal{O}((\Delta\xi)^r,(\Delta\eta)^r).\end{aligned} \tag{A.3}$$

Now we analyze the first term of (A.3). By using Taylor series expansion (2.4) with discontinuous points in Proposition 2.2, we can obtain

$$\begin{aligned}\textit{First term}=&\frac{1}{\Delta\xi}\sum_{l=-L_1^\xi}^{i_D}a_l^\xi(E_{i+l,j}-E_{i,j})\left(\frac{\partial y}{\partial\eta}\right)_{i+l,j}+\frac{1}{\Delta\xi}\sum_{l=i_D+1}^{L_2^\xi}a_l^\xi(E_{i+l,j}-E_{i,j})\left(\frac{\partial y}{\partial\eta}\right)_{i+l,j}\\=&\sum_{l=-L_1^\xi}^{i_D}a_l^\xi\left(\sum_{q=1}^{\infty}l^q\frac{(\Delta\xi)^{q-1}}{q!}\left(\frac{\partial^q E}{\partial\xi^q}\right)_{i,j}\right)\left[\left(\frac{\partial y}{\partial\eta}\right)_{i,j}+\sum_{\tilde{q}=1}^{\infty}l^{\tilde{q}}\frac{(\Delta\xi)^{\tilde{q}}}{\tilde{q}!}\left(\frac{\partial^{1+\tilde{q}}y}{\partial\eta\partial\xi^{\tilde{q}}}\right)_{i,j}\right]\\&+\sum_{l=i_D+1}^{L_2^\xi}a_l^\xi\left[\sum_{q=1}^{\infty}l^q\frac{(\Delta\xi)^{q-1}}{q!}\left(\frac{\partial^q E}{\partial\xi^q}\right)_{i,j}+\sum_{q=1}^{\infty}(l-i_D)^q\frac{(\Delta\xi)^{q-1}}{q!}\left(\frac{\partial^q E}{\partial\xi^q}\right)_{i_A,j}^{R-L}\right]\\&\times\left[\left(\frac{\partial y}{\partial\eta}\right)_{i,j}+\sum_{\tilde{q}=1}^{\infty}l^{\tilde{q}}\frac{\Delta\xi^{\tilde{q}}}{q!}\left(\frac{\partial^{1+\tilde{q}}y}{\partial\eta\partial\xi^{\tilde{q}}}\right)_{i,j}+\sum_{\tilde{q}=1}^{\infty}(l-i_D)^{\tilde{q}}\frac{\Delta\xi^{\tilde{q}}}{\tilde{q}}\left(\frac{\partial^{1+\tilde{q}}y}{\partial\eta\partial\xi^{\tilde{q}}}\right)_{i_A,j}^{R-L}\right],\end{aligned}$$

https://doi.org/10.4208/cicp.250614.060215a Published online by Cambridge University Press

Notice that

$$\sum_{l=-L_1^\xi}^{L_2^\xi} a_l^\xi \left(\sum_{q=1}^{\infty} l^q \frac{(\Delta\xi)^{q-1}}{q!}\left(\frac{\partial^q E}{\partial\xi^q}\right)_{i,j}\right)\sum_{\tilde{q}=1}^{\infty} l^{\tilde{q}}\frac{(\Delta\xi)^{\tilde{q}}}{\tilde{q}!}\left(\frac{\partial^{1+\tilde{q}} y}{\partial\eta\partial\xi^{\tilde{q}}}\right)_{i,j}$$
$$=\sum_{q=1}^{\infty}\sum_{\tilde{q}=1}^{\infty}\left(\sum_{l=-L_1^\xi}^{L_2^\xi} a_l^\xi l^{q+\tilde{q}}\right)\frac{(\Delta\xi)^{q+\tilde{q}-1}}{q!\tilde{q}!}\left(\frac{\partial^q E}{\partial\xi^q}\right)_{i,j}\left(\frac{\partial^{1+\tilde{q}} y}{\partial\eta\partial\xi^{\tilde{q}}}\right)_{i,j}=\mathcal{O}((\Delta\xi)^r)$$

and

$$\sum_{l=i_D+1}^{L_2^\xi} a_l^\xi\left[\sum_{q=1}^{\infty} l^q\frac{(\Delta\xi)^{q-1}}{q!}\left(\frac{\partial^q E}{\partial\xi^q}\right)_{i,j}\sum_{\tilde{q}=1}^{\infty}(l-i_D)^{\tilde{q}}\frac{\Delta\xi^{\tilde{q}}}{\tilde{q}}\left(\frac{\partial^{1+\tilde{q}} y}{\partial\eta\partial\xi^{\tilde{q}}}\right)_{i_A,j}^{R-L}\right]$$
$$=\sum_{l=i_D+1}^{L_2^\xi} a_l^\xi\left[\sum_{q=1}^{\infty} l^q\frac{(\Delta\xi)^{q-1}}{q!}\left(\frac{\partial^q E}{\partial\xi^q}\right)_{i,j}(l-i_D)^k\frac{\Delta\xi^k}{k!}\left(\frac{\partial^{1+k} y}{\partial\eta\partial\xi^k}\right)_{i_A,j}^{R-L}\right]+\mathcal{O}(\Delta\xi^{k+1})$$
$$=\frac{\Delta\xi^k}{k!}\left(\frac{\partial E}{\partial\xi}\right)_{i,j}\left(\frac{\partial^{1+k} y}{\partial\eta\partial\xi^k}\right)_{i_A,j}^{R-L}\sum_{l=i_D+1}^{L_2^\xi} a_l^\xi l(l-i_D)^k+\mathcal{O}((\Delta\xi)^{k+1}).$$

By using the relations (2.8) and getting the main terms of the errors, we obtain

$$\begin{aligned}
\textit{First term}=&\left(\frac{\partial E}{\partial\xi}\right)_{i,j}\left(\frac{\partial y}{\partial\eta}\right)_{i,j}+\frac{\Delta\xi^k}{k!}\left(\frac{\partial E}{\partial\xi}\right)_{i,j}\left(\frac{\partial^{1+k} y}{\partial\eta\partial\xi^k}\right)_{i_A,j}^{R-L}\sum_{l=i_D+1}^{L_2^\xi} a_l^\xi l(l-i_D)^k\\
&+\frac{(\Delta\xi)^{k-1}}{k!}\left(\frac{\partial y}{\partial\eta}\right)_{i,j}\left(\frac{\partial^k E}{\partial\xi^k}\right)_{i_A,j}^{R-L}\sum_{l=i_D+1}^{L_2^\xi} a_l^\xi(l-i_D)^k\\
&+\frac{(\Delta\xi)^k}{k!}\left(\frac{\partial^2 y}{\partial\eta\partial\xi}\right)_{i,j}\left(\frac{\partial^k E}{\partial\xi^k}\right)_{i_A,j}^{R-L}\sum_{l=i_D+1}^{L_2^\xi} a_l^\xi(l-i_D)^k+\mathcal{O}((\Delta\xi)^r)+\mathcal{O}((\Delta\xi)^{k+1})\\
=&\left(\frac{\partial E}{\partial\xi}\right)_{i,j}\left(\frac{\partial y}{\partial\eta}\right)_{i,j}+\mathcal{O}((\Delta\xi)^{\min\{r,k\}})+\frac{(\Delta\xi)^{k-1}}{k!}\left(\frac{\partial y}{\partial\eta}\right)_{i,j}\left(\frac{\partial^k E}{\partial\xi^k}\right)_{i_A,j}^{R-L}\sum_{l=i_D+1}^{L_2^\xi} a_l^\xi(l-i_D)^k.
\end{aligned}\tag{A.4}$$

Substituting (A.4) into (A.3), we can obtain the error of A_E

$$\begin{aligned}
(e_{A_E})_{i,j}=&\frac{(\Delta\xi)^{k-1}}{k!}\left(\frac{\partial y}{\partial\eta}\right)_{i,j}\left(\frac{\partial^k E}{\partial\xi^k}\right)_{i_A,j}^{R-L}\sum_{l=i_D+1}^{L_2^\xi} a_l^\xi(l-i_D)^k+E_{i,j}(\widetilde{I}_x)_{i,j}\\
&-\frac{(\Delta\xi)^{k-1}}{k!}\left(\frac{\partial E}{\partial\eta}\right)_{i,j}\left(\frac{\partial^k y}{\partial\xi^k}\right)_{i_A,j}^{R-L}\sum_{m=i_D+1}^{M_2^\xi} b_m^\xi(m-i_D)^k+\mathcal{O}((\Delta\xi)^{\min\{r,k\}},(\Delta\eta)^r).
\end{aligned}\tag{A.5}$$

https://doi.org/10.4208/cicp.250614.060215a Published online by Cambridge University Press

Then, (4.9) can be obtained by substituting (2.13) into (A.5) and noting that

$$\left(\frac{\partial E}{\partial y}\right)_{i_A,j} = \left(\frac{\partial E}{\partial y}\right)_{i,j} + \sum_{q=1}^{\infty} (i_D)^q \frac{(\Delta\xi)^q}{q!} \left(\frac{\partial^q}{\partial \xi^q}\left(\frac{\partial E}{\partial y}\right)\right)_{i,j}.$$

References

[1] S. D. Rango and D.W. Zingg. Aerodynamic computations using a higher-order algorithm. *AIAA paper 99-0167*, 1999.

[2] S. D. Rango and D. W. Zingg. Further investigation of a higher-order algorithm for aerodynamic computations. *AIAA paper 2000-0823*, 2000.

[3] J.A. Ekaterinaris. High-order accurate, low numerical diffusion methods for aerodynamics. *Progress in Aerospace Sciences*, 41:192–300, 2005.

[4] Z.J. Wang, Krzysztof Fidkowski, and etal. High-order cfd methods: current status and perspective. *Int. J. Numer. Meth. Fluids*, 00:1–42, 2012.

[5] M.R. Visbal and D.V. Gaitonde. On the use of higher-order finite-difference schemes on curvilinear and deforming meshes. *J. Comput. Phys.*, 181:155–185, 2002.

[6] J. Casper, C.W. Shu, and H. Atkins. Comparison of two formulations for high-order accurate essentially nonoscillatory schemes. *AIAA Journal*, 32:1970–1977, 1994.

[7] J.E. Castillo, J.M. Hyman, M.J. Shashkov, and S. Steinberg. The sensitivity and accuracy of fourth order finite-difference schemes on nonuniform grids in one dimension. *Computers Math. Applic.*, 30:41–55, 1995.

[8] C.W. Shu. High-order finite difference and finite volume weno schemes and discontinuous galerkin methods for cfd. *Int. J. Comput. Fluid Dynamics*, 17:107–118, 2003.

[9] T.H. Pulliam and J.L. Steger. On implicit finite-difference simulations of three-dimensional flow. *AIAA Paper 78-10*, 1978.

[10] P.D. Thomas and C.K. Lombard. The geometric conservation law-a link between finite difference and finite volume methods of flow computation on moving grids. *AIAA paper 78-1208*, 1978.

[11] P. D. Thomas and C. K. Lombard. Geometric conservation law and its application to flow computations on moving grids. *AIAA Journal*, 17(10):1030–1037, 1979.

[12] H. Zhang, M. Reggio, J.Y. TršŠpanier, and R. Camarero. Discrete form of the gcl for moving meshes and its implementation in cfd schemes. *Computers and Fluids*, 22 (1):9–23, 1993.

[13] M. Lesoinne and C. Farhat. Geometric conservation laws for flow problems with moving boundaries and deformable meshes, and their impact on aeroelastic computations. *Comput. Methods Appl. Mech. Eng.*, 134:71–90, 1996.

[14] H. Guillard and C. Farhat. On the significance of the geometric conservation law for flow computations on moving meshes. *Comput. Methods Appl. Mech. Eng.*, 190:1467–1482, 2000.

[15] P. Geuzaine, C. Grandmont, and C. Farhat. Design and analysis of ale schemes with provable second-order time-accuracy for inviscid and viscous flow simulations. *J. Comput. Phys., 191 (2003), pp. .*, 191:206–227, 2003.

[16] D.J. Mavriplis and Z. Yang. Construction of the discrete geometric conservation law for high-order time accurate simulations on dynamic meshes. *J. Comput. Phys.*, 213 (2):557–573, 2006.

[17] J. Sitaraman and J.D. Baeder. Field velocity approach and geometric conservation law for unsteady flow simulations. *AIAA Journal*, 44(9):2084–2094, 2006.

https://doi.org/10.4208/cicp.250614.060215a Published online by Cambridge University Press

[18] S. Etienne, A. Garon, and D. Pelletier. Geometric conservation law and finite element methods for ale simulations of incompressible flow. *AIAA Paper 2008-733*, 2008.
[19] D.J. Mavriplis and C.R. Nastase. On the geometric conservation law for high-order discontinuous galerkin discretizations on dynamically deforming meshes. *J. Comput. Phys.*, 230:4285–4300, 2011.
[20] B. Sjogreen, H. C. Yee, and M. Vinokur. On high order finite-difference metric discretizations satisfying gcl on moving and deforming grids. Technical report, Lawrence Livermore National Laboratory, LLNL-TR-637397, 2013.
[21] C. Farhat, P. Geuzainne, and C. Grandmont. The discrete geometric conservation law and the nonlinear stability of ale schemes for the solution of flow problems on moving grids. *J. Comput. Phys.*, 174:669–694, 2001.
[22] L. Formaggia and F. Nobile. Stability analysis of second-order time accurate schemes for ale-fem. *Comput. Methods Appl. Mech. Eng.*, 193:4097–4116, 2004.
[23] K. Ou and A. Jameson. On the temporal and spatial accuracy of spectral difference method on moving deformable grids and the effect of geometry conservation law. *AIAA Paper 2010-5032*, 2010.
[24] X. Deng, Y. Jiang, M. Mao, H. Liu, and G. Tu. Developing hybrid cell-edge and cell-node dissipative compact scheme for complex geometry flows. *Science China*, 56(10):2361–2369, 2013.
[25] T. Nonomura, N. Iizuka, and K. Fujii. Freestream and vortex preservation properties of high-order weno and wcns on curvilinear grids. *Computers and Fluids*, 39:197–214, 2010.
[26] X. Deng and H. Zhang. Developing high-order weighted compact nonlinear schemes. *J. Comput. Phys.*, 165:22–44, 2000.
[27] X. Deng. High-order accurate dissipative weighted compact nonlinear schemes. *Science in China (Series A) x*, 45 (3):356–370, 2002.
[28] X. Deng, X. Liu, and M. Mao. Advances in high-order accurate weighted compact nonlinear schemes. *Advances in Mechanics*, 37 (3):417–427, 2007.
[29] G.S. Jiang and C.W. Shu. Efficient implementation of weighted eno schemes. *J. Comput. Phys.*, 126:202–228, 1996.
[30] X. Deng, M. Mao, G. Tu, H. Liu, and H. Zhang. Geometric conservation law and applications to high-order finite difference schemes with stationary grids. *J. Comput. Phys.*, 230:1100–1115, 2011.
[31] T. Nonomura, D. Terakado, Y. Abe, and K. Fujii. A new technique for finite difference weno with geometric conservation law. *AIAA Paper 2013-2569*, 2013.
[32] X. Deng, Y. Min, M. Mao, H. Liu, G. Tu, and H. Zhang. Further studies on geometric conservation law and applications to high-order finite difference schemes with stationary grids. *J. Comput. Phys.*, 239:90–111, 2013.

https://doi.org/10.4208/cicp.250614.060215a Published online by Cambridge University Press